Engineering Failure Analysis 138 (2022) 106371

Contents lists available at ScienceDirect

Engineering Failure Analysis

journal homepage: www.elsevier.com/locate/engfailanal

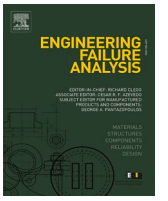

Performance and design of steel structures reinforced with FRP composites: A state-of-the-art review

T. Tafsirojjaman [a], Attiq Ur Rahman Dogar [b], Yue Liu [c,*], Allan Manalo [a], David P. Thambiratnam [d]

[a] Centre for Future Materials (CFM) and School of Engineering,University of Southern Queensland (USQ), Toowoomba QLD-4350, Australia
[b] Department of Civil Engineering, University of Central Punjab, Lahore, Pakistan
[c] Research Institute of Urbanization and Urban Safety, University of Science and Technology Beijing, 30 Xueyuan Road, Beijing, China
[d] School of Civil and Environmental Engineering, Faculty of Science and Engineering, Queensland University of Technology, 2 George Street, Brisbane QLD-4000, Australia

ARTICLE INFO

Keywords:
Steel structures
Strengthening
FRP
Flexure
Compression
Fatigue
Impact
Cyclic Loading
Durability
Prediction models

ABSTRACT

Fiber-reinforced polymer (FRP) composite materials have gained popularity in civil, mechanical, aircraft, and chemical engineering domains due to their superior mechanical properties and durability. They have been used for strength and durability enhancements of civil structures and a wide range of steel structures subject to static (flexure, compression) and dynamic (fatigue, impact, and seismic) loads have been strengthened and retrofitted. The strength enhancement provided by FRP composites to steel structures depends on several parameters including fiber types, fiber orientations, number of fiber layers, steel section types (geometry and grade), member slenderness etc. Although the superior properties of FRP are sometimes affected by severe environmental conditions that the structures are exposed to, these adverse effects can be minimized. This paper provides a comprehensive review of various techniques to improve the performance and design of steel structures using FRP composites. Strength prediction models under a range of loading and environmental conditions are presented in this single document for the evaluation and safe design of FRP strengthened steel structures and thereby minimise their vulnerability to failure.

1. Introduction

Steel structures are the most commonly used structures due to their many advantages including high strength to weight ratio, industrial applications, ease of transportation, and construction [1]. During their service lives these structures may need strengthening/retrofitting due to changes in the building usage or building code requirements. Also, the structures may undergo severe deterioration due to fatigue loads and aggressive environmental effects leading to their premature failure. It is important to select suitable strengthening/retrofitting materials and evaluate the effects of influencing parameters to improve the performance of steel structures. In the past, the steel structures were upgraded by welding external steel plates to the existing structure, but this method was rendered unsuitable due to increased weight, difficulty in application, and susceptibility to corrosion and fatigue damages [2]. An

* Corresponding author.
E-mail addresses: tafsirojjaman@usq.edu.au (T. Tafsirojjaman), attiq.dogar@ucp.edu.pk (A. Ur Rahman Dogar), yueliu@ustb.edu.cn (Y. Liu), allan.manalo@usq.edu.au (A. Manalo), d.thambiratnam@qut.edu.au (D.P. Thambiratnam).

https://doi.org/10.1016/j.engfailanal.2022.106371
Received 2 November 2021; Received in revised form 6 April 2022; Accepted 26 April 2022
Available online 30 April 2022

excellent alternative for upgrading structures is the use of fiber-reinforced polymer (FRP) composite materials which have been increasingly preferred due to higher strength to weight ratios [3,4], extremely low-self weight [5,6], easy installation and application [7,8] as well as good durability [9,10]. In addition to civil structures, FRPs are also preferred in aeronautical, mechanical, and materials engineering fields due to their superior properties.

FRP is a composite material consisting of fibers embedded in resin. The fibers contribute to the mechanical strength of the FRPs, whereas the resin helps in the transfer and distribution of stresses between the fibers. Based on the type of fibers used, there are several types of FRPs including carbon, glass, basalt, and aramid FRPs named as CFRP, GFRP, BFRP, and AFRP, respectively [11]. Among these FRPs, CFRP has the highest strength and deformation resistance, but its drawbacks include higher costs, anisotropy, and susceptibility to galvanic corrosion [12]. GFRP is relatively cheaper compared to other types of FRPs but it has lower long-term strength due to stress rupture as well as lower alkaline and humidity resistance [11]. AFRP has higher strength against static and impact loads, however, its use is limited due to manufacturing and construction difficulties, lower long-term strength as well as their sensitivity to ultra-violet (UV) radiation [13]. BFRP exhibits high tensile strength, good durability, and higher resistance to environmental conditions including corrosion, UV radiations, acids, and high temperatures [14]. There are two types of resins: thermoplastic and thermosetting polymers where thermosetting polymers are preferred as they have higher rigidity, higher thermal, and dimensional stability as well as good resistance against chemical and electrical actions [11]. The fibers and resin can be combined to form FRP laminates, dry fibers, sheets, or rods that can be bonded to the steel structure either by adhesives, fasteners, or clamps. Applications of FRP in various types of structures have already been demonstrated including normal [15-19] and lightweight [20,21] concrete structures, steel structures [22-24], steel–concrete composite structures [25-28] masonry structures [29,30] and timber structures [31,32].

The selection of the suitable type of FRPs for strengthening or retrofitting applications depends on several factors including the applied loads, required strength, service conditions, economy of construction, and types of materials in the existing structures. In addition, parameters related to the mechanical properties and application mechanisms of FRPs also influence the effectiveness of the strengthening. Recently, Siddika et al. [33] summarized the superior performance of FRP strengthened concrete structures in a literature study along with challenges associated with FRP strengthening. To fill the literature gap in FRP strengthening of steel structures and to aid designers and researchers to select an optimal strengthening scheme, a comprehensive literature review on the behaviour of FRP strengthened steel structures in a range and combination of parameters will be useful. Holloway and Cadei [34] highlighted the problems encountered by FRP strengthened steel structures during their service lives, such as bond behaviour between steel and FRP, the durability of FRP composites, and the effect of pre-stressing the FRP plates on strengthening effectiveness. In another study, Shaat et al. [35] provided a review on retrofitting of steel structures with FRPs and highlighted the improvements in fatigue life of bridge girders, techniques to avoid debonding failure, and durability of FRP retrofitted steel structures. Zhao and Zhang [36] categorized the various bond strength testing methods into four categories and recommended the type of tests that can be employed for examining the bond-slip relationship between FRP and steel. In addition, their review paper includes strengthening steel hollow sections in compression, flexure, and fatigue. Similarly, Teng et al. [37] conducted a detailed literature review on the bond behavior between FRP and steel, and the strengthening of steel structures in flexure, fatigue, and the confinement effect of steel hollow sections and concrete-filled steel tubes. They also recommended future studies on durability and fire resistance of FRP strengthened steel structures and strength enhancement of steel structures against blast and impact loadings.

During the past few years, significant studies have been conducted to improve the performance of steel structures under a range of failure modes including flexure [38-50], compression [51-60], impact [61-70], seismic [71-78] as well as fatigue [79-86]. These studies revealed that the effectiveness of FRP strengthening depends on a number of parameters including type of strengthening technique and configuration [47,48], the number of FRP layers and their orientations [43,44,53,57,58,60], slenderness of the steel sections [39,41,55,57,59], types of FRPs and their moduli of elasticity [38,42], and initial imperfections in the steel members [56]. During their service lives, steel structures often require strengthening and/or retrofitting and the selection of an optimal strengthening/retrofitting scheme is imperative for meeting the desired objectives. To help future designers and researchers to select a suitable strengthening scheme, a detailed literature review of the latest studies in this area was carried out and the findings are presented in this paper along with a discussion on the influencing parameters based on the loading conditions. Steel structural members are commonly used as beams and columns in buildings and bridges where flexural, fatigue and compressive stresses are induced in these members. Also, the failure statistics of metallic bridges [87] indicated that buckling and fatigue are their most common failure modes. Strengthening/retrofitting against flexural, compressive, and fatigue loads are therefore covered in this literature review in detail. In addition, steel members are prone to external extreme events such as impact loads from traffic and blasts, as well as seismic loads due to earthquakes. Despite the increased occurrence of these extreme loadings, no previous literature review has covered the strengthening of steel structures against these loads, to the best of the authors' knowledge and this is the first comprehensive review on these important topics. Furthermore, exposure to aggressive environmental conditions affects the durability of FRP strengthened steel structures [88]. Hence the parameters that influence durability have also been discussed in the present paper. Strength prediction models of FRP strengthened steel structures under a range of failure modes and service conditions have also been summarized in this single document to enable their safe designs and minimise their vulnerability to failure.

2. FRP strengthening of steel members under static loads

During their service lives, steel structural members are generally subjected to three types of static loads i.e., tensile, compressive, and flexural loads. Since the nature of applied loads is different, the response of steel members to each type of load will also be different with different failure modes. Typically, steel tension members fail either in yielding in the gross-section, fracture in the net section (bolted/riveted connection), or in the block shear mode depending on which strength is the lowest [89]. However, under both

compression and flexural loads, steel members can either fail under local or global buckling [90]. Local buckling (LB), which could occur at any cross-section of a member depending on its width-to-thickness ratio, results in a reduction in the stiffness of the member against global buckling. Global buckling, on the other hand, depends on the boundary conditions, un-braced length, and radius of gyration of the steel member. Global buckling in the form of lateral-torsional buckling (LTB) can be caused by flexural forces or in the form of flexural buckling (FB), torsional buckling (TB), or flexural torsional (FTB) buckling by compressive forces. As with local buckling limitations, design codes specify the limiting values that specify whether the global buckling would be elastic or inelastic. Since the strengthening of steel members is to reduce the possibility of triggering a failure mode under the loading that a member is subjected to, divisions have been made as per the types of stresses in the steel members. The next sections will discuss the strengthening options that can be employed to improve the resistance against local and global buckling.

2.1. Local buckling

Design codes such as AISC 360–16 [91] and Eurocodes [92] have specified limiting width-to-thickness (plate slenderness) ratios for the plates elements in steel cross-sections under both compressive and flexural loads. These limiting plate slenderness values specify whether a cross-section will reach its full plastic capacity (compact section), or the cross-section plate elements will buckle locally before (slender section) or after (non-compact) the onset of yielding. During their service lives, these cross-section elements need to be strengthened against local buckling to either enhance the capacity of a steel section to plastic capacity and/or improve the plastic hinge behaviour to enhance the ductility of the member. Wrapping steel sections with FRPs can delay the occurrence of local as well as global buckling and can also increase the plastic hinge size, thus contributing to enhanced load, rotation, and energy dissipation capacities as well as reduced strain demands [93]. The strengthening effectiveness depends on several factors including the employed fiber orientations, modulus of the FRPs as well as their location.

Application of FRPs can either be done by orientating the fibers in the direction parallel to the axis of the member (longitudinal, L), perpendicular to the axis (transverse/hoop, T) (Fig. 1), or at an angle to the member's axis. The employed orientation of fibers affects the strengthening effectiveness of FRPs. Al-Sayyed [94] conducted finite element analysis of I-section beams with different web height to thickness ratios (49.8, 107.8, 148, and 296.2) and bonded FRP strips at mid-height of these webs. Web buckling behaviour significantly improved with these longitudinally oriented FRPs and the maximum increase in critical load was observed for class-4 (slender) sections as the critical buckling and ultimate loads increased by 20–60% and 29% respectively. Effect of the wrapping scheme to improve the local and global buckling behaviour of double channel members of a truss moment frame was also evaluated by Ekiz et al. [93] and Tawil et al. [95]. They conducted cyclic tests on local buckling (LB) and lateral-torsional buckling (LTB) prone members and assessed the improvement in plastic hinge behaviour of these sections using CFRPs. In the first type of specimen, only flange was reinforced with four (4L) and six (4L + 2 T) while the other type of specimen was fully wrapped with six (3L + 3 T) CFRP layers. They concluded that longitudinally oriented fibers were beneficial in improving the local buckling behaviour whereas a combination of longitudinally and transversely oriented fibers was beneficial for improving the LTB behaviour. Overall, all the wrapping schemes delayed the onset of LB as well as LTB and increased the size of the plastic hinge region.

Interestingly, it has been found that the mismatch in elastic moduli of the steel and FRPs have proven to be beneficial in improving the local buckling behaviour of the steel sections. FRPs with lower modulus are moderately stressed at the onset of local buckling and their entire flexural capacity is available for bracing the underlying steel members [96]. Accord and Earls [40] used GFRPs to strengthen compression flanges of cantilever I-section beams. The primary aim of their investigation was to assess the feasibility of GFRPs in performance enhancement as the low modulus GFRPs will be stressed less at the onset of local buckling compared to the CFRPs and this will lead to enhanced flexural resistance. They concluded that longitudinally oriented GFRPs provide adequate ductility to the steel members, however, no comparisons with CFRPs were made. The comparison between the effectiveness of CFRPs and GFRPs was conducted by Ragheb et al. [97] as they used uni-directional (UD) and bi-oriented (0/90) degree oriented GFRP layers with longitudinal, transverse, and shear moduli of 30, 4.5, and 5.0 and 24.0, 24.0, 5.0 respectively and the same for CFRP layers were CFRP layers were 120, 4.5, and 5.0 and 66.0, 66.0, 5.0. They found a higher rotation index for GFRP strengthened (25%) beams compared to CFRP strengthened beams (12%) with the bi-oriented sheets resulting in a higher rotation index compared to uni-directional (UD) sheets.

The impact of the location/placement of the FRPs was experimentally assessed by Harries et al. [96] through concentric cyclic tests on WT sections. They strengthened the local buckling prone webs of the WT sections with two different strengthening schemes: (1) using a single 50.8 mm wide and 1.4 mm thick strip and (2) using two 25.4 mm wide and 1.4 mm thick strips. Both the strips had the

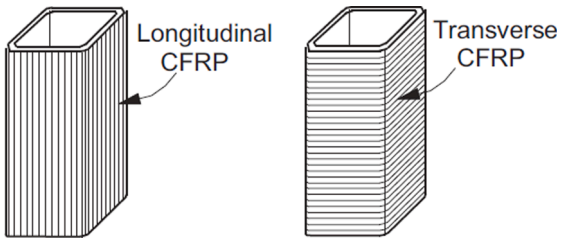

Fig. 1. Orientations of fibers in longitudinal and transverse directions.

same area and centroid and the length of the specimen was 356 mm. The capacity of the specimens increased by 4–14%, and the specimen with two 25.4 mm wide strips performed better. Accord and Earls [40] also assessed the effect of location of GFRPs on improvement in ductility of cantilever I-section beams using finite element analysis. They considered isotropic material behavior considering only longitudinal modulus of elasticity and concluded that placing the GFRP strips away from the web-flange junction result in improved ductility of the members. On the other hand, Ragheb et al. [97,98] considered the orthotropic material behaviour in elastic and inelastic stability analysis of CFRP strengthened steel elements in compression and flexure. Contradicting with the results of Accord and Earls [40], they concluded that CFRP strips placed closer to the web-flange junction are more effective in increasing the ultimate loads. They also concluded that the shear modulus of the FRPs had a significant influence on restraining the local buckling of the flanges while the longitudinal and transverse moduli did not contribute much. However, for web strengthening, transverse modulus has a significant effect when the strips are placed at the mid-height of the web. If the strips are placed on the web near the web-flange junction, shear modulus also has a significant impact.

2.2. Global buckling

Only a small amount of FRP reinforcement is required for strengthening steel members against local buckling, as sufficient stability can be achieved by a small bracing force. However, for global buckling, this small amount is insufficient for strengthening as global buckling depends on the overall length, radius of gyration, and support conditions of the member. This insufficiency of small amount of FRP reinforcement against preventing global buckling was demonstrated by Harries et al. [96] by using the same amount of FRP reinforcement on the same section with different lengths. The first strengthening scheme was the use of a single 50.8x1.4 mm thick strip and the second scheme was the use of two 25.4x1.4 mm thick strips. For each type of strengthening scheme, two samples were prepared with varying lengths. These two lengths were 356 mm and 1664 mm resulting in web local buckling (WLB) prone and flexural torsional buckling (FTB) prone specimens. As the strength gain reduced from 1.14 for WLB prone specimens to 0.97 for FTB prone specimens with CFRP strengthening, they concluded that the small amounts of FRPs, usually suitable for strengthening against local buckling, are not sufficient for preventing global buckling. Therefore, a relatively larger amount of FRPs is required to strengthen the member against global buckling. In this review study, strengthening effectiveness against global buckling has been treated separately for flexural and compression members.

2.2.1. Flexural members

The behaviour and failure mode of members in flexure depends on the cross-sectional shapes. There can be three types of cross-sectional shapes i.e., closed sections with the same radius of gyration about both axes (circular or square hollow sections), closed sections with different radii of gyration about both axes (rectangular hollow sections), and open cross-sections (W, C, and angle sections, etc). Closed sections that are symmetrical about both the axes can either fail by yielding or by local buckling of the

Table 1
Effects of fiber orientations on bending strengths of members with different slenderness ratios [39,43,44,51,52,99].

Section type	λ_s	$\sigma_y^{(s)}$ (N/mm^2)	Fibre orientation	$M_p^{(s)}$ (kN.m)	M_u (kN.m)	$M_u^{(cs)}/M_u^{(s)}$	Reference
Compact	24.0	479	–	1.48	1.55	–	[32]
	33.2	327	–	15.06	15.35	–	[36]
	24.2	479	HHL	1.46	1.60	1.03	[32]
	33.2	327	LHL	12.86	20.34	1.33	[36]
	33.2	327	HHL	12.86	20.06	1.30	[36]
	33.2	327	LLH	12.86	20.40	1.33	[36]
	24.0	479	HHLL	1.48	2.24	1.45	
Non-compact	50.3	380	–	4.76	5.30	–	
	80.0	455	–	6.70	5.80	–	[32]
	50.3	380	LLH	4.76	8.00	1.51	
	79.1	455	HHL	6.78	7.77	1.34	[32]
	78.0	455	HHLL	6.88	8.45	1.46	[32]
Slender	122.1	470	–	4.47	3.32	–	
	139.1	457	–	3.66	2.69	–	[44]
	163.9	457	–	3.07	2.13	–	
	147.8	468	L	3.61	2.98	1.11	[44]
	141.2	468	LH	3.78	3.66	1.36	[44]
	116.5	470	HHL	4.71	5.24	1.58	[32]
	138.3	457	HHL	3.68	4.32	1.60	[44]
	124.1	470	HHLL	4.37	5.30	1.60	
	138.7	457	LHLH	3.65	4.48	1.67	[44]
	172.1	468	HLHL	3.06	4.08	1.92	
	179.2	470	HHLL	2.95	3.91	1.84	
	180.1	468	HHHL	2.92	3.23	1.52	

compression flanges. For closed sections with different radii of gyration about the 2 axes and for open sections, lateral-torsional buckling (LTB) can cause the failure of the members in addition to local buckling [91]. LTB occurs because of the compression on one side, which tends to buckle the member and the tension on the other side which tends to keep the member straight resulting in combined torsion and buckling of the member. Depending on the member's slenderness and bracing conditions, these members can utilize their full plastic moment capacity, undergo buckling after a part of the cross-section has yielded (inelastic buckling), or buckle even before the attainment of yield stress (elastic buckling). The strengthening of flexural members, in either case, depends on several factors including the amount of fiber reinforcement, fiber orientations, tensile modulus of the FRPs, and the slenderness of the member.

2.2.1.1. Amount of fibers and fiber orientations and fiber moduli. The amount of fibers and their orientations play a critical role on the effectiveness of FRP strengthening of members. Both the critical elastic buckling loads and the ultimate loads increase with an increase in the number of FRP layers and/or thickness of fiber reinforcements due to the restrictions on the buckling deformations provided by fiber reinforcements [60]. Fibers are normally oriented in two directions: (i) transverse (T) or hoop (H) direction and (ii) longitudinal (L) direction (Fig. 1). Transverse or hoop layers, oriented perpendicular to the longitudinal axis of the member, exert a circumferential restraint on the buckling of the compression side wall of the steel member. Longitudinal fibers, oriented parallel to the longitudinal axis of the beam, enhance the capacity of the tension side wall of the member [39]. In addition, there can be a third orientation in which fibers are oriented at an angle to the longitudinal axis of the member.

For the closed sections susceptible to local buckling and yielding, a combination of the hoop and longitudinal layers is necessary to improve the capacity of the section. Haedir et al. [39,51,52], Tafsirojjaman et al. [99] and Kabir et al. [43,44] conducted detailed experimental tests on compact (C), non-compact (NC), and slender (S) CHS beams to assess the effect of the amount of fiber reinforcements and orientations of the fibers on strength improvement. The cross-section slenderness (λ_s), steel yield stress ($\sigma_y^{(s)}$), fiber orientation, plastic moment capacity of the steel section ($M_p^{(s)}$), experimental ultimate moment capacity (M_u), and the ratio of capacities of composite and steel sections ($M_u^{(cs)}/M_u^{(s)}$) are presented in Table 1. For the same number of fiber layers, more longitudinal layers result in higher moment capacity, however, more hoop layers result in increased rotational capacity. For slender beams strengthened with HHLL and HLHL orientations, the capacity of the beams increased even more than the plastic capacity of the section, whereas beams with HHHL had lower capacities than the previous two. Overall, it is recommended to use LHL layers for better strength enhancement and moisture control.

Rasheed et al. [100] conducted numerical investigations on the effect of the amount of fiber reinforcement and fiber layup on critical bending moments of LTB prone steel-FRP hybrid beams with thin-walled rectangular cross-sections. They studied the effect of stacking fiber layers on either one or both sides of individual plate elements of the section. They concluded that maximum critical bending moment is achieved when the fibers are stacked at one side of the cross-sectional plate elements compared to the plate elements in the middle of FRPs. They also plotted critical bending moments for different angles of fiber orientations from 0° to 90° with increments of 5° and concluded that maximum capacity is achieved for ply-layup of [20/-20/20/20/-20/20/ST] (Fig. 2). For such an angle, maximum lateral and torsional effectiveness is obtained resulting in optimal strength enhancement, but it is recommended to conduct further studies to verify the effect of inclined fiber layups.

For open sections prone to LTB, researchers suggested converting the open cross-section into a closed section and wrapping it with FRPs. Deng et al. [101] converted a cruciform-shaped open section of a buckling restrained brace (BRB) with GFRP tubes and then wrapped it with GFRP (Fig. 3). They evaluated the effect of two parameters i.e. thickness and wrapping angle of the GFRP layer. Two different layer thicknesses of 3 mm and 6 mm were used along with two wrapping schemes i.e., transverse and mixed (one transverse layer and one at an angle of 45° to the transverse layer). They concluded that a thickness of 6 mm was necessary to wrap the BRBs effectively and the wrapping angle had no significant effect as the GFRP tube was effective in the longitudinal direction and wrapping layers in the transverse direction. Global buckling was avoided with this strengthening scheme, but the specimen failed by local buckling at the ends, for which they recommended to use GFRP tubes with better local stability. Selvaraj and Madhavan [47]

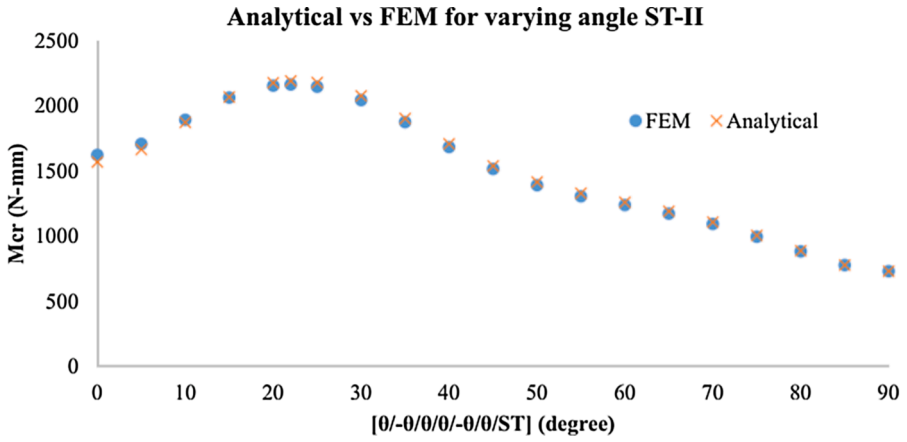

Fig. 2. Variation of moment capacity with change in fiber layups [100].

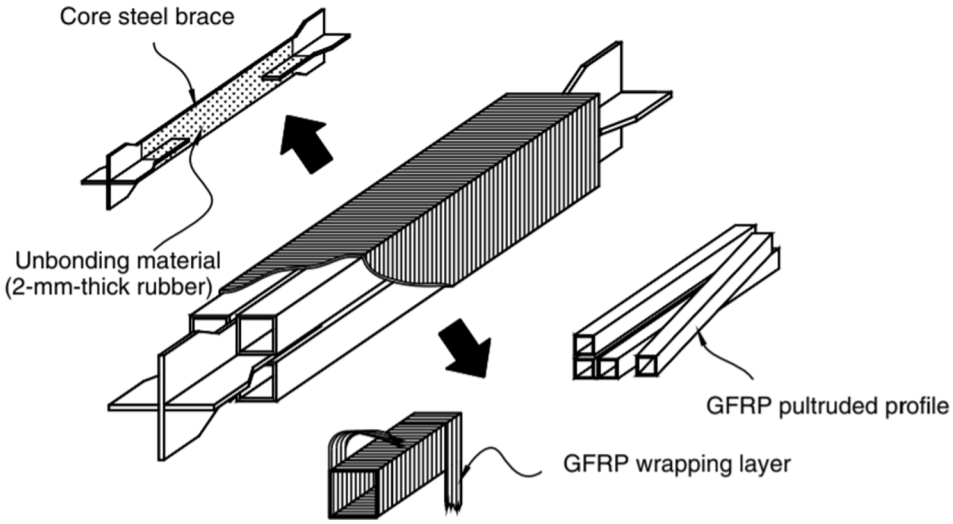

Fig. 3. Proposed strengthening scheme for open sections Deng et al [101].

strengthened deep C-sections in two different ways; (i) CFRP wrapping around the perimeter (SS) and (ii) closing of C-sections with cardboard and wrapping with CFRP (CS) using both uni-directional (U) and bi-directional (B) layers. They concluded that the surface strengthening technique was not suitable to resist LTB as the SS-1U and SS-1B had increased ultimate load capacities of 7.1% and 14.52% respectively. Similarly, the application of unidirectional CFRPs on closed sections was not suitable due to the tearing of stitching fibers. However, using a single bi-directional layer improved the moment capacity by 33.64% compared to the un-strengthened specimen and a combination of uni and bi-directional layers (1U + 1B + 1U + 1B) increased the moment capacity up to the plastic moment capacity.

Modulus of elasticity of the FRP also affects the strengthening effectiveness as the material with a higher elastic modulus (E) attracts more stresses. When bonded with FRPs of higher tensile moduli, stresses in the underlying steel element reduce leading to improved section capacity. Also, the stiffness of the composite section is increased leading to reduced deflections. However, FRPs with higher tensile moduli have lower values of ultimate strains which may affect the post-elastic ductility and ultimate strength of the beam.

Kabir et al. [43] conducted numerical investigations on the effect of CFRP modulus on CHS strengthened beams. They used three CFRPs with varying moduli of elasticity of 150, 210, and 552 GPa and used the same layer orientation of LHL. The yield load capacity increased by 22% as the CFRP modulus increased from 150 GPa to 552 GPa alongwith stiffness of the specimen. Siwoski and Siwoska [48] tested steel I-section beams with CFRP plates of two different moduli of elasticity i.e. 160 GPa and 207 GPa. An increase in the elastic modulus did not affect the ultimate strength of the beam but the yield flexural capacity improved by 5%. However, the increase in elastic modulus of beams reduced the ductile performance of beams in the post-elastic range. Ghafoori and Motavalli [38] used normal (100–200 GPa), high (200–400 GPa), and ultra-high modulus (greater than 400 GPa) CFRPs for strengthening of I-section beams. They found that the increase in the modulus of elasticity of CFRP resulted in increased elastic stiffness of the beam and reduced tensile stresses in the bonded flange. However, the interfacial shear stresses also increased which led to premature debonding of the laminates. This premature debonding can be eliminated by using mechanical clamps or epoxies with high ductility.

2.2.1.2. Slenderness of underlying steel member. As the slenderness of the steel member as well as that of individual steel plate elements of the cross-section increases, the susceptibility of the member to buckling deformations also increases. Wrapping with FRPs exerts a restraint on these buckling deformations due to which the percentage gain in strength also increases with increasing plate or member slenderness as shown in Table 1. For sections that do not undergo elastic buckling (either local or global), the effectiveness of FRP strengthening is minimal.

Siddique and El Damatty [41] conducted numerical investigations on built-up sections with slender flanges and compact webs. The load and deflection improvement factors for a simply supported beam under four-point loads were 1.34 and 5.09 for the compact beam with a 19 mm thick GFRP plate, whereas the same improvement factors for slender beams were 1.85 and 8.71 respectively. Haider et al. [39] conducted tests on compact, non-compact, and slender CHS sections as per AS4100 standards [102]. The strength gain variation was directly proportional to the increase in cross-section slenderness and amount of fiber reinforcement with 92% strength gain in sections with the highest slenderness and maximum amount of fiber reinforcements.

2.2.2. Compression members

Steel members subjected to compressive forces can fail either in local buckling or one of the three modes of global buckling i.e. flexural buckling (FB), torsional buckling (TB), or flexural torsional buckling (FTB), depending on the cross-section shape [91]. Flexural buckling occurs in the members about the axis with the largest slenderness ratio and/or least radius of gyration. Torsional buckling occurs in doubly symmetric cross-sections about the longitudinal axis. Flexural torsional buckling, the simultaneous bending

and twisting of the members, occur in un-symmetrical cross-sections with one axis of symmetry. Overall, similar to flexural members, the strengthening effect of FRPs for compression members depends on the amount and orientations of fibers, the tensile modulus of the fibers, and the slenderness of the plate elements or members. There is, however, an additional factor due to initial imperfections which also has a significant effect on compression members.

2.2.2.1. Amount of fibers, fiber orientations, and fiber moduli. The compressive strength enhancement of steel members with FRPs is directly related to number of layers [103-105]. The effect of fiber orientations, however, depends on whether the compression member is short or long. Effects of fiber orientation on strength enhancement of short columns with and without slender cross-sections are presented in Table 2. Shaat and Fam [58,106] strengthened non-slender (class-2) short and long SHS columns with CFRPs. They strengthened short columns with 1H, 2H, 1L, and 1L1H layers and long columns with 1L, 3L, and 5L layers. It was concluded that transverse layers were more effective in increasing the capacity of short columns and a maximum strength gain of 18% was achieved with two transverse layers. For the long columns, strength gain was in the range of 13–23% with the maximum strength gain for three longitudinal layers. Although the strength gain increases with the increase in layers, however, the results were affected by initial out-of-straightness of the long columns. To assess the exclusive contribution of the number of layers, they conducted a finite element study [55] and found a direct relationship between the number of CFRP layers and strengthening effectiveness. However, no comparison was drawn for longitudinal and transverse layers for long columns.

Kumar and Senthil [53] used four different fiber orientations i.e. 1L, 1H, 1L1H, and 2L2H on CHS columns with a slenderness ratio of 25. They concluded that transverse layers were more effective than the longitudinal fibers as they prevented the lateral expansion of the steel tubes. The authors recommended using one hoop layer for a 10% strength increase and a combination of the hoop and transverse layers for a 25–35% increase in strength compared to the bare member. Haedir and Zhao [103] also recommended using a combination of longitudinal and transverse fibers for optimal strength and ductility enhancements.

Imran et al. [60] conducted experimental and numerical investigations of CFRP strengthened short SHS CFS columns under axial static compression loading to see the effect of CFRP wrapping orientations. Contrary to previous studies of Shaat and Fam [58] and Kumar and Senthil [53] under axial static loading, they found that longitudinally oriented fibers outperformed the transverse fibers. This is due to the fact that their cross-sections were slender, and the longitudinally oriented fibers delayed the onset of local buckling as the failure mode also changed from local buckling for the control specimen to yielding for the specimen with two layers. They, however, also recommended using a combination of transverse and longitudinal fibers to control the membrane stresses developed in both directions. Moreover, the CFRP was applied in SHSs and CHSs by wet-layup technique with adhesive by Kumar and Senthil [53], Shaat and Fam [58] and Imran et al. [60]. First, the steel specimens were sandblasted to make the surface rough and achieve a better bond between FRP and steel surface. Then the sandblasted surface was cleaned with acetone to remove any debris on the surface. Before applying the adhesive, they applied an adhesion promoter to the acetone treated surface to enhance the bond strength and cured for 15 min. Then the two-part saturated resin was mixed as per manufacturer guided ratio and applied on both surfaces of the FRP using a rib-roller to ensure that the FRPs were fully saturated with adhesive. Then the saturated FRP was placed on the steel specimen and the rib-roller was moved along the FRP thoroughly to achieve a good finish. For the case of multi-layer FRP strengthening, the strengthened specimen was allowed to cure for about 60 min before the applying the the subsequent layers. All strengthened specimens

Table 2
Effects of fiber orientation on strength of short columns.

Section	Application	λ_s	$\sigma_y^{(s)}$ (N/mm^2)	Fibre orientation	$P_u^{(s)}$ (kN)	$P_u^{(cs)}/P_u^{(s)}$
SHS [58]		23.1	380	–	396.30	
				H	455.00	1.15
				HH	467.30	1.18
				L	431.00	1.09
				LH	455.00	1.15
	Short and long columns			H	427.80	1.08
				HH	440.00	1.11
				L	433.00	1.09
				LH	440.00	1.11
CHS [53]		25.95	412	–	342.30	
				L	345.10	1.01
	Long column			H	384.40	1.12
				LH	422.20	1.23
				LLHH	469.30	1.37
SHS [60]		50.84	359	–	169.40	
				H	248.00	1.46
	Short column			L	267.90	1.58
				HL	281.60	1.66
				HL	370.30	2.19
				HHLL	443.20	2.62

Table 3
CFRP strengthening for fatigue strength improvement.

Reference	Strengthening/Repairing scheme	Mechanical properties of strengthening scheme	Recommendation
Nakumara et al. [83]	(1) CFRP (2) Drill-holes (DH) (3) Drill-holes with 1 (DHS) & 5 (DHM) CFRP layers (4) Combination of 2 & 3 (DHMS)	CFRP: T_U = 2990 E = 206 Dia of drill holes = 25 mm	Fatigue life improvement compared to non-repaired specimen: DH = 1.6times DHM = 5times DHMS = 80times
Chen et al. [113]	Effects of weld toe radius Number of CFRP layers Modulus of strengthening materials	CFRP: T_U = 4180 E = 200, 250, 300, 400, 500, 600, 650 Weld toe radius = 0.5, 1, 2, 3 mm No. of CFRP layers = 1, 3, 5	Weld toe radius and number of CFRP layers have significant effect on CFRP strengthening effectiveness. For weld toe radius of 1 mm, fatigue life improved by 20, 45, and 60 % with 1, 3 and 5 layers respectively. Maximum fatigue life was achieved with lowest weld to radius of 0.5 mm.
Yue et al. [114]	(1) BR –5L CFRP layers with 3 additional hoop layers at the end of CFRP layers. BCR1 – 5L CFRP layers with 1 additional hoop layers at the end of CFRP layers and stiffener cut of 30 mm. BCR2 – 5L CFRP layers with 3 additional hoop layers at the end of CFRP layers and stiffener cut of 30 mm.	CFRP: T_U = 4306 E = 245	No. of fatigue cycles Un-strengthened = 561, 579 BR = 2830 BCR-1 = 1224 BCR-2 = 3230 BCR-2 is the most effective strengthening scheme.
Liu et al. [81]	Strengthened steel plate having a central notch with three different configurations of longitudinal CFRP patches bonded on either single or both sides. Case A = Bare steel plate with a central notch. Case B = Steel plate fully covered by composites. Case C = Steel plate with two separate patches straddling the central notch. Case D = Steel plate with partially bonded CFRP sheets around the central notch.	CFRP type-1 T_U = 3800 E = 240 CFRP type-2 T_U = 2650 E = 640	Maximum strength gain was achieved for double side repairs with fatigue life increase ratio of:Case B (Type-1 CFRP) = 2.7Case B (Type-2 CFRP) = 7.9Case C (Type-2 CFRP) = 5.0Case D (Type-2 CFRP) = 4.7 Fatigue life increases by covering full width of plate with high modulus CFRPs.
Taljsten el at. [117]	Strengthened web plates of an old bridge girder with a central notch using two types of CFRP plates. The details of specimen are: A = unstrengthened B = Strengthened with CFRP type-1 C = Strengthened with CFRP type-2 D = Type B with pre-stressed (15 kN) CFRP laminates E = Type C with pre-stressed (12 kN) CFRP laminates	CFRP type-1 T_U = 2000 E = 155 CFRP type-2 T_U = 2500 E = 260	Fatigue life of the specimens B and C improved by 2.45 and 3.74 times respectively and the fatigue life of the corresponding specimens with pre-stressed laminates (D and E) improved considerably as the specimens didn't fail.
Hu et al. [111]	Strengthened three different high-strength steel members with different chemical compositions using CFRP laminates.	CFRP: T_U = 4710 E = 435 Steel: E = 201 T_y = 390, 485, and 805	Steel members with a high grain size obtained by micro-alloying exhibited higher fatigue life. At the same stress levels, steel specimens with higher tensile strength exhibited higher fatigue life in both the un-strengthened and strengthened specimens.
Feng et al. [110]	Studied the fatigue behaviour of CFRP strengthened cracked steel plates at temperature ranges of -40^{O}C to 60^{O}C. Major focus was on the behaviour of different types of adhesives.	CFRP: T_U = 4710 E = 435 Steel: E = 204 T_y = 330	Overall, the fatigue life improved in the range of 2 to 3.4 times. Glass transition temperature (T_g) is the most critical factor at higher temperatures i.e. temperatures greater than 45 °C and the resin properties reduce above this temperature lowering the fatigue life.

T_u = Tensile strength (MPa), E = Elastic Modulus (GPa), T_y = Yield strength (MPa).

were allowed to cure for at least 14 days at room temperature before the testing. Recently, Wu and Zhi [54] conducted tests on GFRP reinforced CHS long columns with slender sections and considered three different winding angles (30°, 45°, and 90°). The strength gain was in the range of 26.8% to 32.5% and the maximum strength gain was achieved with the winding angles of 30° and that transverse layers (winding angle of 90^{O}) did not contribute much.Based on Euler's column theory according to which the strength of a long column depends on the rigidity of the member (EI) rather than the material strength. Ritchie et al. [56] conducted experimental tests on long I-shaped columns strengthened with CFRPs of different moduli in the range of 168 GPa to 430 GPa. They concluded that the percentages in strength gain (12%-29%) increased with the increase in E, but this strength gain was highly non-linear and it reaches a plateau at higher values of modulus of elasticity (E). Also, the lateral deflections of the column reduced with an increase in E.

2.2.2.3. Slenderness of underlying steel member. Shaat and Fam [59] conducted experiments on HSS columns with varying slenderness ratios of 46, 70, and 93 strengthened with high modulus (313 GPa) CFRP plates. Although the load capacities decreased with the increase in column slenderness, the strengthening effectiveness increased and the percentage gain in strength improved by 6%, 35%, and 71% for the columns with the slenderness ratios of 46, 70, and 93 respectively. For the failure modes, the un-strengthened column failed by buckling and the columns with slenderness ratios of 46 and 71 failed by debonding of CFRP before buckling and close to the peak load respectively. For the column with a slenderness ratio of 93, crushing of the CFRP occurred after the peak load indicating full strength utilization of CFRPs. The authors suggested a further study on the effect of transverse wrapping on HSS columns. An increase in CFRP strengthening effectiveness with an increase in column slenderness has also been verified by other authors [55,57,60].

2.2.2.4. Initial imperfections. Initial imperfection, also known as out-of-straightness of a member, is a lateral deflection that is already present in a compression member at the time of erection. Due to this initial lateral deflection, bending moments are generated in a member in addition to compressive stresses resulting in increased buckling deformations and lower capacity of the members. It has been found that the initial imperfections can affect the experimental results and these values must be evaluated and incorporated before conducting tests for comparisons of strengthening effectiveness [58]. Shaat and Fam [55] found out that the effectiveness of CFRP retrofitting increases with an increase in initial imperfection but for a given CFRP reinforcement ratio, there is a specific value of initial imperfection beyond which the strength gain becomes constant. Ritchie et al. [56] studied the effect of initial out of straightness on CFRP strengthening effectiveness and grouped I-shaped slender columns into three categories based on initial imperfections i.e. small, average, and large. The corresponding average initial imperfections were 0.31, 1.68, and 2.55 mm. The strength of both the control and strengthened columns reduced with an increase in initial imperfection, however, the percentage gain in strength increased with increasing initial imperfections.

3. FRP strengthening of steel members under dynamic loads

3.1. Fatigue loads

Most steel structures, especially bridges, tanks, pipelines, and crane beams are subjected to cyclic loads due to moving traffic which varies in magnitude as well as position/direction. Due to this, there will be variation in stresses and cracks may develop and propagate near connections even due to stresses significantly lower than yield stresses and lead to loss of resistance over time known as fatigue failure. As the opening and progress of cracks are alleviated by tensile stresses, materials possessing high tensile strength that can induce compressive stress in the underlying material can increase the fatigue strength efficiently. Also, materials with high stiffness decrease the stress range around the crack tips developed due to fatigue loadings. Owing to high tensile strength and modulus of elasticity (E), FRP is an optimal strengthening option. FRPs increase the fatigue life of structures by impeding crack growth, reducing effective stresses around crack tips as well as crack opening displacements [107]. The effectiveness of the strengthening with FRPs against fatigue loadings has been well demonstrated by several studies [23,37,108-112] and depends on the number and arrangement of FRP layers, the elastic modulus of the FRPs, and prestressing levels of the FRPs. The strengthening schemes, mechanical properties of strengthening schemes, and recommendations of the researchers are given in Table 3.

An increase in the number of CFRP layers increases the fatigue strength of steel structures, rigidity of the strengthening system and therefore reduces the crack opening displacement. Nakumara et al. [83] conducted fatigue tests on welded web gusset joints and

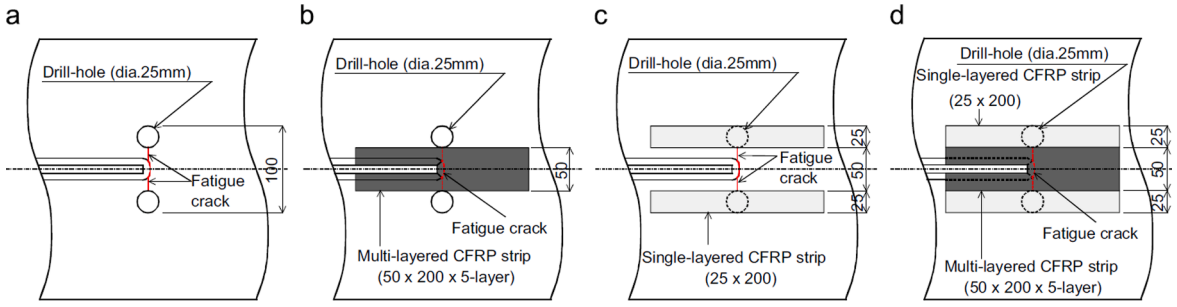

Fig. 4. Combination of FRPs and drill holes (a) DH (b) DHM (c) DHS (d) DHMS [77].

studied the effect of the number of layers as well as the combination of CFRPs with drill holes (Fig. 4). The technique of drilling holes at the ends of fatigue cracks was traditionally employed to reduce the stress concentrations at the crack tips. They used only drill holes (DH), a combination of drill holes and 5 layers of CFRPs (DHM), a combination of drill holes and a single layer of CFRPs over the drill holes (DHS), and a combination of DHS and DHMS (Fig. 4). They concluded that this technique of using a combination of drill holes and CFRPs yields better results as compared to repairing with only CFRPs, however, the crack opening displacement increases due to the presence of drill holes. In another study by Chen et al. [113], the effect of the number of CFRP layers on non-load-carrying cruciform welded joints was examined. They used one and three layers of CFRPs with a tensile strength of 4182 MPa and E of 250 GPa and used two stress ranges i.e. 180 MPa and 216 MPa. Their numerical studies indicated that an increases in the number of CFRP layers, modulus of CFRP layers and decrease in radius of weld toes increase the fatigue life of the strengthened structure. To eliminate the effect of FRP debonding on strengthening effectiveness, Yue et al. [114] strengthened the steel girders with five longitudinal layers and wrapped the ends of these longitudinal layers with one and three additional hoop layers. The sample with three additional hoop layers outperformed the sample with one hoop layer as the failure initiation was significantly delayed.

FRPs with higher elastic modulus reduces the stresses at the crack tips and thereby improve the fatigue life. Also, as the crack propagates under fatigue loadings, higher modulus FRPs, with high stiffness have a considerable restraining effect on crack growth and propagation. Increase in fatigue life and reduction in crack propagation have been well demonstrated by research studies [115,116]. Liu et al. [81] applied CFRPs on one and both sides of steel plates with notches with normal (E of 240 GPa and tensile strength of 3800 MPa) and high (E of 640 GPa and tensile strength of 2650 MPa) modulus CFRPs. Both the normal and high modulus CFRPs increased the fatigue life but using higher E increased the fatigue life by 3 times. The failure mode also changed from debonding for normal modulus to fiber breakage for high modulus. To improve the fatigue life of old metallic bridges, Taljsten et al. [117] showed that CFRP laminates with higher elastic modulus i.e. 260 GPa resulted in improved fatigue life performance as compared to laminates with lower modulus i.e. 155 GPa.

Pre-tensioning the FRPs induces compressive stresses in the steel substrate impeding the crack growth and improving the fatigue life [108,115]. As per the studies of Taljsten el at. [117], prestressing the CFRP laminates affected the crack propagation and fatigue life more than the elastic modulus. The pre-tensioning force required to improve the fatigue life, however, depends on the static and fatigue strength of the bonded joint, and future studies on varying stress ranges and pre-stressing levels are needed to develop proper guidelines.

Feng et al. [110] studied the effect of extreme temperature ranges (-40 ^{O}C to 60^{O}C) on the strengthening effectiveness of CFRPs. They found out that crack propagation speed is affected by the temperature and this speed reduces with the decrease in temperature thus improving the fatigue life. The crack propagation speed was constant in the temperature range of 20^{O}C to 40 ^{O}C and then increases again with increasing temperature. At the temperature of 60^{O}C, the fatigue life becomes half to that of at 20^{O}C. Even at this temperature, the fatigue life of the strengthened specimen was twice than that of the unstrengthened specimen.

3.2. *Impact loads*

Structural steel members are vulnerable to impact loads from vehicles, ships, airplanes, rock-falls, debris impacts, etc. During an impact event, the mass of the impact body moving with a velocity imparts energy to the steel member, and sufficient energy absorption capacity is required to withstand this impact load. Initial studies on the impact behaviour of CFRP strengthened steel members were conducted by Zubaidy et al. [69,70] where they compared the bond strength between CFRP plates and steel under static and a range of impact loads. Their results indicated that the CFRP-steel bond behaves considerably well under impact loads compared to that under static loads. A similar increase in bond strength was obtained for the steel and ultra-high-modulus CFRPs by Al-Mosawe et al. [118]. Generally, the behavior of steel members under impact loads is investigated in terms of mean residual force and axial and lateral displacements. Mean residual force is the dynamic capacity of the member and gives an important estimate of the member's strength during an impact event. Different parameters that affect the strength under impact loads include types of fibers, amount of fiber reinforcements, orientations of fibers, support conditions, and axial pre-loading.

When steel members are strengthened with FRPs, their stiffnesses increase and result in higher impact resistance (or force) with reduced deflections [63]. Alam and Fawzia [61] tested bare, two sides strengthened, and four sides strengthened SHS columns under initial impact velocities ranging from 4 m/s to 10 m/s while keeping the impact mass constant. The initial impact force caused by the initial impact velocity was greater in two and four sides strengthened columns and increased with an increase in impact velocity. The mean residual force, however, was higher for four sides strengthened column, but was similar in the two sides strengthened column and the bare column indicating the inadequacy of two sides strengthening. After changing both the impact velocity and impact mass, Alam and Fawzia [61] concluded that four sides strengthening was necessary for strength enhancement as indicated by improved mean residual force and reduced deflections. The outcomes in columns strengthened on two sides were similar to those in the bare steel columns.

Fiber properties i.e., type and modulus of FRPs also affect the initial impact force and the response of strengthened steel tubes. Change in the properties, especially the elastic modulus, affects the initial stiffness of the members resulting in increased impact force and reduced deflection. Alam et al. [62] tested CFRP and GFRP reinforced CHS beams under transverse impacts and compared the effectiveness of both. They found out that CFRP wrapping was most effective due to increased mean residual forces and reduced lateral deflections. The effect of change in FRP material was also studied by Batuwitage et al. [64,65] who investigated the effects of GFRP, normal modulus CFRP and high modulus CFRP on initial impact force and lateral displacement. They concluded that the initial impact force of GFRP is lower than that of CFRPs and amongst the CFRPs, the initial impact force increases with an increase in modulus. Compared to the bare CHS, the axial deflections reduced by 9 mm, 12 mm, and 18 mm with GFRP, normal modulus CFRP and high

modulus CFRP, respectively.

There is a direct relationship between the amount of fiber reinforcement (thickness or number of layers) and strengthening effectiveness. By varying the number of CFRP layers from one to five, Alam and Fawzia [61] found that the initial impact force did not change considerably but the mean residual force increased considerably. Also, an increase in the number of layers from one to five resulted in significant reductions in the axial and lateral displacements. In another study, Alam et al. [62] also reported that increase in the number of layers enhances the strengthening effectiveness, however, they recommended using a combination of longitudinal and hoop layers to improve both the global and local deformation capacities. By making realistic vehicle impact models on CFRP strengthened CHS columns, Alam et al. [68] found out that bare and strengthened columns with hoop layers had similar strength under impact loads and the addition of longitudinal layers resulted in significant strength enhancement (Fig. 5). Kadhim et al. [63] also confirmed the decrease in lateral deflections with increasing CFRP thickness but the thickness above 2 mm did not have a notable effect on deflection reduction. In an experimental study on CFRP strengthened SHS beams, Kadhim et al [67] studied the effects of CFRP thicknesses of 1.2 mm, 2.4 mm, 3.6 mm, and 4.8 mm and found out that increasing the thickness reduced the lateral deflections and maximum reduction was observed for 4.8 mm thick CFRP.

For effective strengthening, a combination of hoop and longitudinal layers is required for proper confinement of the column and longitudinal layers. Longitudinal layers provide stability against global deformations but their contribution in reducing local deformations is limited. small. [39]. Alam et al. [62] investigated the effect of fiber orientations and concluded that LHL layers performed better than LLL and HLH layers (Fig. 6). They also found that specimens reinforced with three longitudinal layers had the least performance, even compared to HL layers, as there were no hoop layers to confine them. They also concluded that for the same number of layers, more longitudinal layers result in lesser deformations as demonstrated by the results with LHL and HLH layers.

To study the effects of support conditions, Alam and Fawzia [61] tested columns under three types of boundary conditions i.e. fixed–fixed, fixed-pinned, and pinned–pinned. The initial impact force was not affected by the boundary conditions, but the mean residual forces increased considerably for fixed–fixed conditions. For the pinned–pinned conditions, the impact durations increased, and the impact resistance decreased. Overall, the columns with fixed–fixed conditions performed better in terms of energy dissipation capacity and reduced lateral deflections.

Axial pre-loading also affects the strengthening effectiveness and an increase in axial pre-load results in increased deflections and reduced strength. Alam and Fawzia [61] varied the axial pre-loads from 0% to 70% of the column's ultimate capacity before applying the impact load. The bare steel column, two sides strengthened column and four sides strengthened column failed at axial pre-loads of 50%, 60%, and 70% of their ultimate capacities. All the columns failed by local buckling, the bare and two sides strengthened column failed by outward side buckling while the four sides strengthened column failed by inward and outward buckling at the front and rear sides of the impact location.

3.3. Seismic loads

Rigid and semi-rigid steel frames have been widely used in seismic areas [119,120] where the beam-column connections influence their behaviour. Adequate strength, as well as ductility of the joint, is required to withstand seismic loads, and investigations on the

Fig. 5. Effect of number of layers on impact resistance (a) control (b) HL (c) LHL [68].

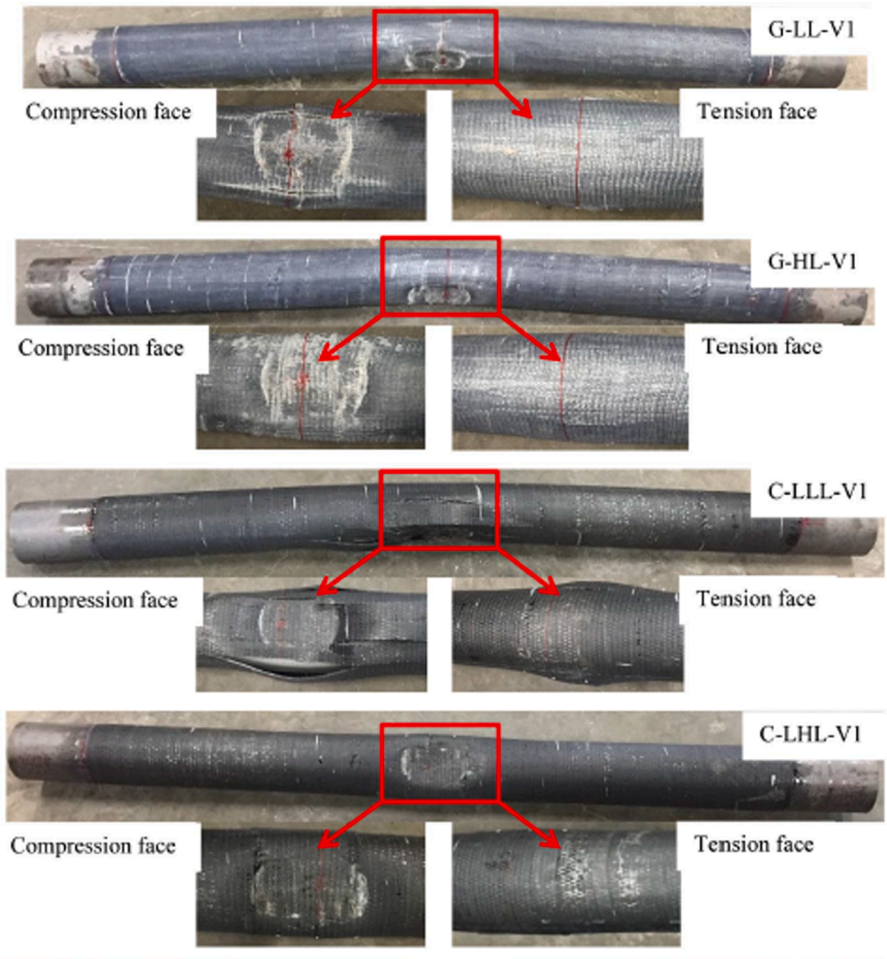

Fig. 6. Effect of layer orientations and number of layers on impact resistance [62].

steel welded connections [121,122] have revealed their inadequacy as they undergo brittle failure due to high-stress concentrations in these joints [121-125]. To improve the ductility of these welded connections, steel plates were traditionally welded to the connections [126,127], but this method has its drawbacks i.e. higher dead load of the structure, reduced fatigue performance of the joint, and difficulty in their application. CFRP wrapping has proved to be a superior alternative for seismic strengthening and rehabilitation of steel structures as it delays the local buckling [128], improves the energy absorption [72], and impact resistance [66] along-with enhancing the fatigue performance of joints [129].

Studies on the seismic strengthening of steel structures with CFRPs are quite few and can be categorized into the behaviour of members and the behaviour of frames. Tafsirojjaman et al. [72] conducted monotonic and cyclic load tests on CFRP strengthened CHSs and found that the moment-deformation behaviour of CFRP strengthened CHS was similar under both monotonic and cyclic loads with a 33% increase in the moment capacity. The energy dissipation capacity, ductility also improved by 18% and 13% respectively along with the increase in rotational capacity from 0.06 rad to 0.08 rad. In another numerical investigation, Tafsirojjaman et al. [76] conducted a parametric study to ascertain the influence of CFRP thickness, the diameter-to-thickness ratio of the CHS (slenderness), and CFRP bond length on its cyclic performance. They found that the CFRP effectiveness increased with increase in thickness as well as slenderness of the member. For the 1100 mm long specimen, a bond length of 400 mm was found to be optimal as lengths more than 400 mm did not contribute much to the strength. Influence of the number of CFRP layers, modulus of CFRP, bond length, and slenderness of the member were also evaluated for RHS steel sections [77]. It was concluded that 3 layers of the CFRP were optimal with no influence of modulus of CFRP. For 1100 mm long specimen, 300 mm was found to be the optimal length. As with CHS sections, the effectiveness of CFRP strengthening of RHS sections also increased with increase in plate slenderness.

In another study, Tafsirojjaman et al. [130] also compared the effectiveness of CFRP and GFRP strengthening on SHS beam-column connections under cyclic loadings using the same type of adhesives. They concluded that the ultimate moment capacity of the connection is better improved by CFRP strengthening as the capacity enhancements were 41.3% and 31.8% with CFRP and GFRP strengthening respectively. On the other hand, GFRP strengthening exhibited better performance in terms of ductility as the ultimate moment capacity was attained at rotations of 0.04 and 0.05 rad for CFRP and GFRP strengthening schemes respectively. In addition to

Table 4
Effect of various durability techniques on strength improvement.

Study	Durability improvement Technique	Exposure condition	Ultimate Load (kN)	$P_u^{(c)}/P_u$	Additional Comments
Seica and Packer [49]	Control		240		Sika Fibers (T = 537 MPa, E = 50350 MPa) Fyfoe fiber (T = 500 MPa, E = 62500 MPa) (Fyfo epoxy-special for underwater curing)
	Sika fiber - Sika epoxy	Standard curing (in air)	279	1.16	
	Fyfo fiber - Fyfo epoxy		305	1.27	
	Sika fiber - Sika epoxy	Underwater curing	260	1.08	
	Fyfo fiber - Fyfo epoxy		278	1.16	
	Sika fiber - Sika epoxy	Underwater curing with additional circumferential nylon ties	266	1.11	
	Fyfo fiber - Fyfo epoxy		290	1.21	
Dawood and Rizkalla [143]	Control		43.7		Adhesive (T = 38 MPa, E = 2980 MPa)
	Bare	1 week wet/1 week dry cycle in a 5% NaCl solution at 38^{O}C for 6 months	23.1	0.53	
	Silane coupling agent		50.4	1.15	
	GFRP		35	0.80	
	Silane + GFRP		58.7	1.34	
Kabir et al. [144]	Control		77.575		Adhesives (Mbrace T = 46 MPa, E = 2860 MPa) (Araldite K630 T = 33 MPa,E = 6500 MPa,) (T = 31.28 MPa,Sikadur E = 4820 MPa,)
	Adhesive-Mbrace	Accelerated corrosion (10% loss of mass) at ambient temperature for 25 days	74.75	0.96	
	Adhesive-Araldite K630		75.82	0.98	
	Adhesive-Sikadur		75.4	0.97	
	Adhesive-Mbrace + GRRP		86.4	1.11	
	Adhesive-Araldite K630 + GFRP		90.2	1.16	
	Adhesive-Sikadur + GFRP		88.5	1.14	
	Adhesive-Mbrace	Accelerated corrosion (10% loss of mass) at 50^{O}C for 25 days	74.25	0.96	
	Adhesive-Araldite K630		75.45	0.97	
	Adhesive-Sikadur		74.6	0.96	
	Adhesive-Mbrace + GRRP		84.25	1.09	
	Adhesive-Araldite K630 + GFRP		87.42	1.13	
	Adhesive-Sikadur + GFRP		86.13	1.11	
Kabir et al. [142]	Control		76.75		Adhesive (T = 46 MPa, E = 2860 MPa) S1 and S2 refer to sample 1 and 2 with different strengths.
	S1-Adhesive + Primer	Accelerated corrosion at ambient temperature for 25 days	75.85	0.99	
	S1-Adhesive + Primer + GFRP		80.5	1.05	
	S2-Adhesive + Primer		95.3	1.24	
	S2-Adhesive + Primer + GFRP		86.3	1.12	
	S1-Adhesive + Primer	Accelerated corrosion at 50 °C for 25 days	73.55	0.96	
	S1-Adhesive + Primer + GFRP		71	0.93	
	S2-Adhesive + Primer		85.4	1.11	
	S2-Adhesive + Primer + GFRP		83	1.08	

moment and rotational capacities, the energy dissipation capacities of the connections also increased by 84.2% with CFRP and by 203.9% with GFRP strengthening.

Welded steel beam-column connections are the most crucial parts in frames as they undergo brittle failure under seismic excitation. Several parameters influence the behaviour of CFRP strengthened steel frames including the number of layers, CFRP thickness, and modulus of CFRP. An increase in the effectiveness of CFRP strengthening with the increase in the number of layers was experimentally observed by Tafsirojjman et al. [75] where the tip lateral displacement decreased by 59% compared to 41% when the number of CFRP layers was increased from 1 to 2. Tip lateral displacement also decreased with increase in thickness [74] and modulus of the CFRP [71]. Tafsriojjaman et al. [71] also conducted detailed experimental studies on three types of CFRP strengthened double-story single-bay steel frames. In the first and second frames, the critical regions of columns and slab plate were strengthened with one and two layers of CFRPs respectively while in the third frame the columns were strengthened with a single layer of CFRP while the plate slabs were strengthened with two layers of CFRP. They deduced that the CFRP strengthening effectiveness increase with the increase in modulus, thickness as well as the number of CFRP layers. They also concluded that an increase in the number of CFRP layers beyond 3 did not significantly affect the strength enhancement.

4. Durability of FRP strengthened steel structures

Although the FRP composites show good environmental performance, the strength and stiffness of the adhesive are generally degraded under severe environmental conditions [131-133]. Exposure to severe environmental conditions i.e. marine/seawater applications and hot/cold weather deteriorate the bond between FRP and steel member and also reduces its ductility [134,135]. In this section, the causes of strength and stiffness reductions under severe environmental conditions are summarized and the parameters that can improve the durability of FRP strengthened systems are discussed.

4.1. High moisture and wet environment

Out of all the environmental threats, severe deterioration of the bonded joint is caused by the penetration of water through diffusion, capillary action through voids and cracks, or absorption through porous adherents. This penetration of water can affect the properties of the adhesive [1,5], facilitate galvanic corrosion and ultimately cause reduced strength and stiffness of the member [132]. Selection of suitable adhesive and use of electric insulator are necessary to improve the durability of structures under marine/seawater environments. Effects of various techniques for durability improvement in seawater conditions are given in Table 4.

For applications where metallic coupling is likely i.e. in marine environments, epoxies that have hydrolyzable linkages (ester bonds) should be avoided [136-138]. The use of organic fiber plies, isolating epoxy film on steel surface, or moisture barrier creates electrical isolation and prevents galvanic corrosion. A comparison between the galvanic corrosion of graphite/epoxy and graphite/vinyl ester composites in seawater revealed that epoxy-based composites performed better to resist galvanic corrosion due to the presence of non-hydrolyzable matrix while the vinyl-ester based composites showed blistering under these conditions [137,139]. Seica and Packer [49] conducted tests on tubular members strengthened with CFRPs and used a special type of epoxy resin with thixotropic nature. This epoxy resin is recommended for use under submerged conditions as it able to keep the resin viscous and within the impregnated fibers. They concluded that such an adhesive is superior to the normal adhesive and also results in improved performance for submerged curing conditions.

CFRP strengthened steel structures are susceptible to galvanic corrosion especially in wet environments due to the potential difference between CFRP and steel and the presence of an electrolyte [140]. In marine environments, the presence of seawater containing salts and minerals and the use of de-icing solutions in bridge applications can serve as a medium for ion exchange between CFRP and steel. To prevent this galvanic corrosion, an electrical insulator in the form of epoxy [138] or an additional GFRP layer [141,142] can be used. Dawood and Rizkalla [143] compared the effectiveness of using additional GFRP layers, pre-treating with silane coupling agents, and a combination of additional GFRP layers and silane coupling agents and concluded that maximum strength is achieved by using a combination of silane coupling agents and GFRP. Kabir et al. [144] evaluated the performance of three different adhesives with varying elastic moduli with and without the inclusion of the additional GFRP layer. They concluded that the addition of the GFRP layer with its higher modulus yields better results. In another study, Kabir et al. [142] demonstrated that the inclusion of GFRP layers along with the combination of adhesives and primer yields the best results. In addition, the durability of the FRP strengthened system is also directly related to the thickness of the steel section [142,144] as well as the FRP [49], number of FRP layers [145], and the diameter of the steel section [144]. However, to develop accurate design factors, it is necessary to conduct more tests with varying section geometries and specimen conditioning alternatives.

4.2. Cold weather

Cold weather has adverse effects on the durability of FRP strengthened steel members as it leads to micro-cracking of the matrix and bond degradation. For effective performance of FRP strengthened steel members under cold weather conditions, the use of an adhesion primer and adhesives with higher elastic modulus can result in enhanced performance. Kabir et al. [146-148] performed a series of experiments to evaluate the improved durability of FRP strengthened steel members. In all their studies, they used acetone to remove the weak layers after sand-blasting the steel members. Before applying the adhesive, they applied an adhesion promoter to the acetone treated surface to enhance the bond strength. Application of this adhesion primer yielded good results as the degradations of strength and stiffness of these FRP strengthened beams reduced as opposed to the untreated beams without primer [146]. In another study,

Kabir et al. [147] compared the effectiveness of two different commercially available adhesives in addition to the application of the adhesion primer. The tensile strength, compressive strength, and elastic modulus of first and second adhesives were 50 MPa, 80 MPa, and 3000 MPa and 30–35 MPa, 105–115 MPa, and 7000–8000 MPa respectively. Although the strength and stiffness degraded with the cold-weather conditioning, the second adhesive with higher compressive strength and elastic modulus performed better in terms of load capacity and deflections, especially in the plastic zone. In their third study, Kabir et al [148] conditioned the beams under cold weather (+3°C) for 12 months as opposed to the cold weather conditioning of 3 and 6 months in the previous two studies. They again used two types of adhesives with the same properties and reported that the adhesive with greater compressive strength and elastic modulus performed better. They also evaluated the effects of section thickness, diameter, modulus of the CFRP, adhesive thickness, and the number of CFRP layers on the durability of strengthened members and concluded that durability increases with the increase in all these parameters. One of the major findings of their study was that the orientation of fibers also affects the strengthening effectiveness, and a combination of longitudinal and hoop layers is necessary for improved durability. Members strengthened with LHL layers performed better than LLH layers for three layers and the difference was negligible for four layers.

For the durability design of FRP strengthened structures, it is imperative to use a strength reduction factor as per the service conditions. The few studies on the effects of cold weather showed large ranges of strengths and deflections for different sections with different thicknesses, diameters, and conditioning periods. Further studies are therefore required to develop a pool of data to derive strength reduction factors for durability designs.

5. Prediction models of FRP strengthened structures

5.1. FRP reinforced CHS under static and dynamic loads

5.1.1. Flexural strength prediction model

Strength enhancement of steel sections reinforced with FRPs depends on the amount as well as properties of the FRP reinforcement. To calculate the strength of the composite steel-FRP section, existing prediction models of steel sections are modified to account for the contribution of FRP reinforcement. Haedir et al. [39] developed the design prediction model of FRP strengthened steel CHS by modifying the slenderness of the steel section. As per the AS4100 [149], the normalized cross-section slenderness (λ_s) of the CHS under bending is calculated using Eq. (1).

$$\lambda_s = \left(\frac{d_s}{t_s}\right)\left(\frac{\sigma_y^{(s)}}{250}\right) \tag{1}$$

where $\frac{d_s}{t_s}$ is the ratio of outer diameter to section thickness of steel and $\sigma_y^{(s)}$ is the yield stress of steel. To account for the presence of FRP reinforcement, the FRP thickness is replaced by an equivalent amount of steel using the modular ratio (β) and fiber strength efficacy (α_m). The fiber strength efficacy takes into account the limited compressive strength contribution of FRPs. Haedir et al. [39] proposed this fiber strength efficiency as 19% based on the proportion of the compressive strength of the cured fibers to the tensile strength of the dry fibers as per the tests of Seica et al. [150]. The transformed thickness ($t_{es}^{(cs)}$) of a number of FRPs layers ($j = 1, 2, \ldots m_{cs}$) to steel can then be calculated using Eq. (2).

$$t_{es}^{(cs)} = \frac{1}{\beta\alpha_m}\sum_{j=1}^{m_{cs}} t_j^{(cs)} = \frac{t_{j=1}^{(cs)} + t_{j=2}^{(cs)} + t_{j=3}^{(cs)} + \ldots\ldots\ldots}{\beta\alpha_m} \tag{2}$$

where β is the ratio of elastic modulus of steel to that of FRP sheet and α_m is calculated using Eq. (3).

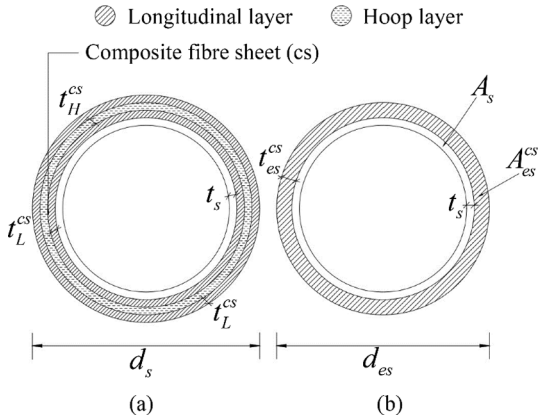

Fig. 7. (a) Composite steel-FRP section (b) transformed section [146].

$$\alpha_m = \frac{0.19\sigma_u^{(cs)}}{\sigma_y^{(s)}}, 0 \leqslant \frac{A_h^{(cs)}}{A_l^{(cs)}} \leqslant 3.0 \tag{3}$$

where $\sigma_u^{(cs)}$ and $\sigma_y^{(s)}$ are the tensile stresses of the fiber sheet and steel respectively and $A_h^{(cs)} \Big/ A_l^{(cs)}$ is the ratio of cross-sectional areas of the hoop and longitudinal layers. Once the transformed thickness is obtained using Eq. (2)., the diameter (d_{es}) and thickness (t_{es}) of the composite FRP-steel section (Fig. 7) can be calculated using Eqs. (4) and (5) respectively.

$$d_{es} = d_{j=0}^{(s)} + 2t_{es}^{(cs)} \tag{4}$$

$$t_{es} = t_s + t_{es}^{(cs)} \tag{5}$$

where $d_{j=0}^{(s)}$ and t_{es} are the outer diameter and thickness of the steel profile respectively.

The cross-section slenderness of the FRP-steel composite section can then be calculated using Eq. (6), which is a modified form of standard Eq. (1).

$$\lambda_{es} = \left(\frac{d_{es}}{t_{es}}\right)\left(\frac{\sigma_y^{(s)}}{250}\right) \tag{6}$$

The bending capacity (M_b)is then calculated by multiplying the section modulus (Z_{ese}) with the yield stress of steel ($\sigma_y^{(s)}$) (Eq. (7)). For the compact cross-section, the section modulus (Z_{ese}) is the plastic section modulus of the equivalent section (S_{es}), whereas the section moduli of the non-compact and slender cross-sections can be calculated using Eqs. (8) and (9) respectively.

$$M_b^{(cs)} = Z_{ese}\sigma_y^{(s)} \tag{7}$$

$$Z_{ese} = Z_{es} + \left\{\left[\frac{(\lambda_{sy} - \lambda_{es})}{(\lambda_{sy} - \lambda_{sp})}\right](S_{es} - Z_{es})\right\} \tag{8}$$

$$Z_{ese} = Z_{es}\sqrt{\left(\frac{\lambda_{sy}}{\lambda_{es}}\right)} \tag{9}$$

where λ_{sp} and λ_{es} are the plastic and yield limits for the plate element slenderness respectively. Haedir et al. [39] demonstrated the accuracy of the developed procedure by comparing the results of the developed model with the test results of Seica et al. [150] (Fig. 8). Both the number and orientation of fiber layers varied between the specimens and the number of reinforcing fiber layers varied between 1 and 4. The comparison suggests the accuracy of the developed model as well as the consideration of fiber strength efficacy (α_m).

Haedir et al. [39] also evaluated the effect of the number of fiber reinforcements on steel sections of constant thickness and varying

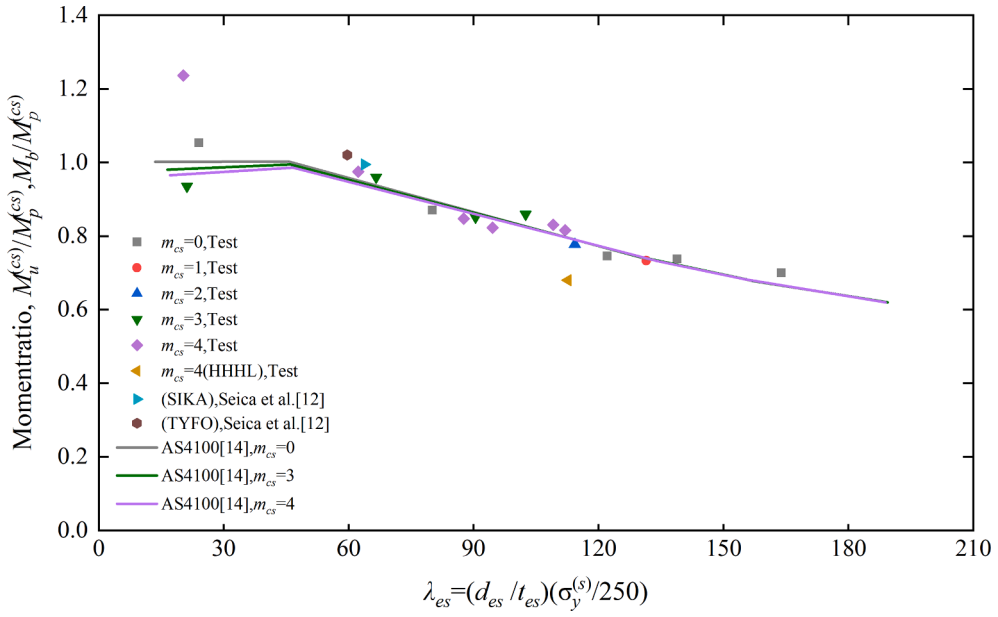

Fig. 8. Comparison of calculated and experimental capacities of CFRP reinforced CHS [39].

diameters using the proposed model. They found that as the amount of fiber reinforcements increase, the plastic moment capacity of the section also increases (Fig. 9). They also demonstrated the accuracy of the proposed model for non-compact sections with fiber orientation different from that of Seica et al. [150].

5.1.2. Compressive strength prediction model

Design equations of CFRP strengthened steel SHS columns were proposed by Shaat and Fam [58] and Bambach et al. [57]. The model proposed by Shaat and Fam [58] is valid only for compact sections ignoring the effects of local buckling along with a non-linear increase in the capacity with an increase in CFRP thickness. Although the model of Bambach et al. [57] considers these parameters, they, however, considered the compact section to be isotropic. To include the effects of CFRP fiber orientations, Imran et al. [60] modified the design equations of Bambach et al. [57] by introducing a proportioning factor (ξ) and the adopted procedure is also similar to the AISI procedure [151]. The axial compressive capacity P_u and the theoretical critical buckling P_{cr} loads of the CFRP strengthened SHS columns can then be calculated using Eqs. (10) and (11), respectively.

$$P_u = 4\rho b t f_y + A_r f_y \tag{10}$$

$$P_{cr} = A_g f_{cr} \tag{11}$$

whereρ,b,t,f_y and A_r are the effective width factor, clear width, thickness, yield stress, and area of the rounded corners of the steel section respectively. The effective width factor ρ can be calculated using Eqs. (12) through (21).

$$\rho = \frac{1 - \frac{0.22}{\lambda_c}}{\lambda_c} \tag{12}$$

$$\lambda_c = \sqrt{\frac{f_y}{f_{cr}}} \tag{13}$$

$$f_{cr} = \frac{k\pi^2 D_t}{t_T b^2} \tag{14}$$

$$D_t = \frac{D_1 D_3 - D_2^2}{D_1} \tag{15}$$

$$D_1 = \frac{E_s t}{1 - v_s^2} + \frac{E_{CE}(t_T - t)}{1 - v_C^2} \tag{16}$$

$$D_2 = \frac{E_s t^2}{2(1 - v_s^2)} + \frac{E_{CE}(t_T^2 - t^2)}{2(1 - v_C^2)} \tag{17}$$

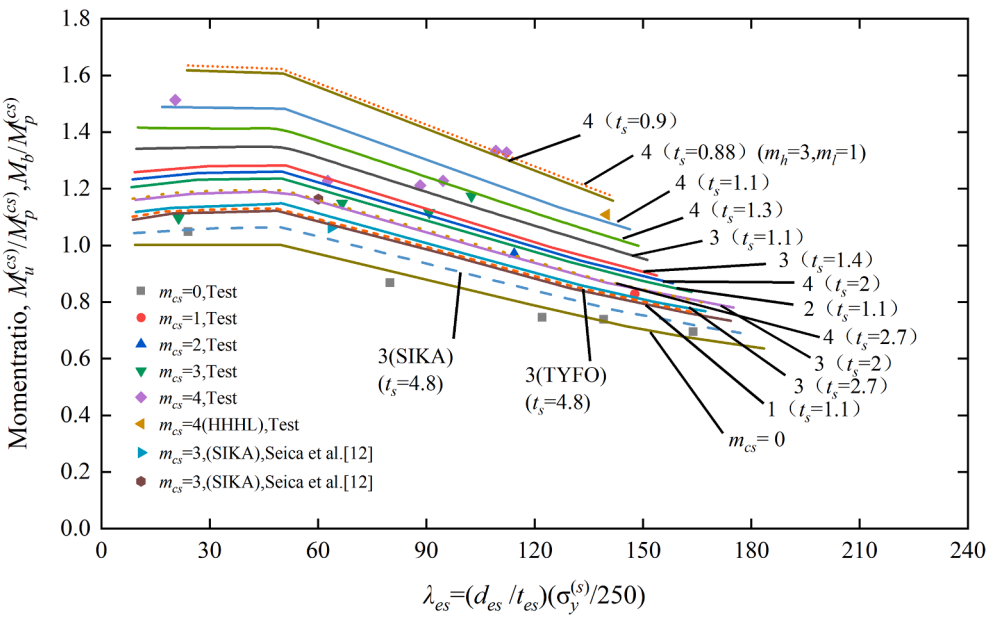

Fig. 9. Design curves for bare and CFRP strengthened CHS in bending [39].

$$D_3 = \frac{E_s t^3}{3(1-\upsilon_s^2)} + \frac{E_{CE}(t_T^3 - t^3)}{3(1-\upsilon_C^2)} \tag{18}$$

$$t_T = t + t_C(N_L + N_T) \tag{19}$$

$$E_{CE} = \frac{N_L E_{1C} + \xi N_T E_{1C}}{N_L + N_T} \tag{20}$$

$$E_{1C} = E_C \nu + E_a(1-\nu) \tag{21}$$

where λ_c is the composite plate slenderness ratio, f_{cr} is the elastic critical buckling stress, k is the elastic buckling coefficient (4 for the stiffened elements), D_t is the flexural rigidity of the composite section recommended by Pister and Dong [152], t_T is the total thickness of the composite section, E_s is the elastic modulus of steel, υ_s is the Poisson's ratio of steel, E_{CE} is the equivalent stiffness of the CFRP composite, υ_C is the Poisson's ratio of CFRP, t_C is the CFRP composite layer thickness, N_L is the number of longitudinal layers,N_T is the number of transverse layers, E_{1C} is the elastic modulus of CFRP in the longitudinal direction, E_C is the elastic modulus of carbon fibers, E_a is the elastic modulus of adhesive, and ν is the fiber volume ratio. The effective width b and rounded corner area of the steel section A_r can be calculated using Eqs. (22) and (23) respectively.

$$b = b_w - 2r \tag{22}$$

$$A_r = A_g - 4bt \tag{23}$$

Based on the properties of CFRP used, Imran et al. [60] recommended a ξ value of 0.8. However, they recommended that future research should be conducted on CFRP strengthened 1 T and 1L tubular columns to calculate a general ξ value. They also proposed a strength reduction factor (ϕ_u) of 0.9 for CFRP strengthened tubular columns which is equal or close to the recommended factors of 0.90 and 0.85 in AS4100 [60] and AS/NZS4600 [153] respectively.

Additionally, Imran et al. [60] also recommended a design procedure for the direct strength method (DSM) which is recommended by AS/NZS4600 [153] and AISI [151] for steel sections. First, they developed DSM-based design strength curves by plotting P_u/P_y against slenderness ratios (λ) calculated using Eq. (24) for a range of sections (Fig. 10). The elastic buckling load (P_{cr}) can be calculated by either using Eq. (11) or through any commercially available finite element software. The axial compression capacity (P_u) of the CFRP strengthened steel tubular columns can be calculated using Eqs. (25) and (26).

$$\lambda = \sqrt{\frac{P_y}{P_{cr}}} \tag{24}$$

$$P_u = \begin{cases} 1.2P_y & for\ \lambda \leqslant 0.52 \\ \left[1 - 0.18\left(\frac{P_{cr}}{P_y}\right)^{0.44}\right]\left(\frac{P_{cr}}{P_y}\right)^{0.44} P_y & for\ \lambda > 0.52 \end{cases} \tag{25}$$

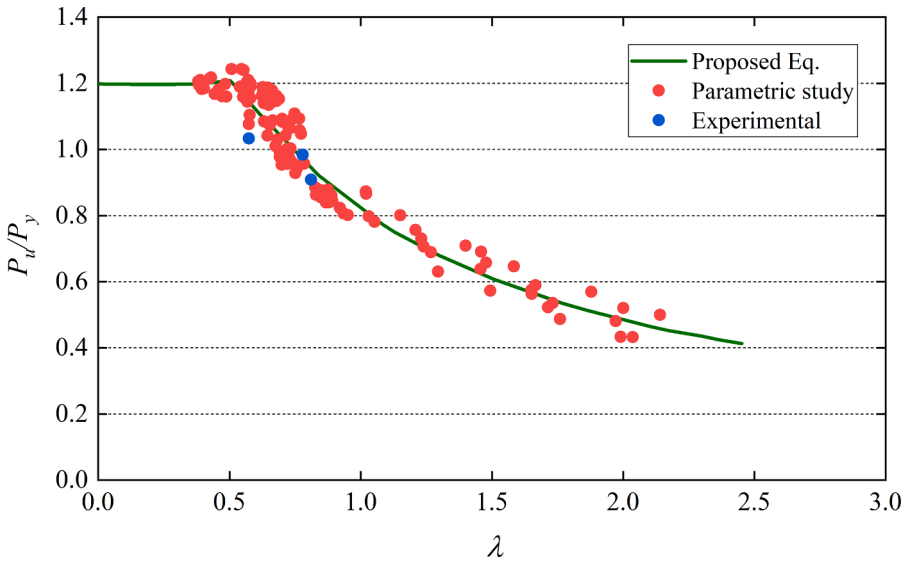

Fig. 10. DSM based design curves [60].

$$P_y = A_g f_y \tag{26}$$

They proposed a strength reduction factor (ϕ_u) of 0.9 for DSM based method also.

In another study, Haedir and Zhao [103] also proposed the strength calculation of CFRP strengthened CHS steel short columns using the equivalent section. They also considered the effects of variation of fiber orientations on axial compressive strength of such columns by using a proportioning factor. The transformed thickness (t_{es}^{cs}) of the section with both the steel and CFRP can be calculated using Eq. (27).

$$t_{es}^{cs} = \eta_L \beta_L t_L^{cs} + \eta_H \beta_H t_H^{cs} \tag{27}$$

where η_L and η_H are the ratios of areas of CFRPs to that of steel, β_L and β_H are the modular ratios related to the longitudinal and hoop fibers respectively, and t_L^{cs} and t_H^{cs} are the thicknesses of the longitudinal and hoop CFRP fibers respectively. The values of β_L and β_H can be calculated using Eqs. (28) and (29) respectively.

$$\beta_L = \frac{E_{1t}^{cs}}{E^s} = \frac{E_{1c}^{cs}}{E^s} > 1.0 \tag{28}$$

$$\beta_H = \frac{E_{2t}^{cs}}{E^s} = \frac{E_{2c}^{cs}}{E^s} < 1.0 \tag{29}$$

whereE_{1t}^{cs},E^s,E_{1c}^{cs},E_{2t}^{cs}, E_{2c}^{cs} are Young's moduli of longitudinal fibers in tension, steel, longitudinal fibers in compression, transverse fibers in tension, and transverse fibers in compression respectively. To account for the effect of fiber orientations, the elastic modulus of the fibers in the hoop direction is transformed into the elastic modulus of longitudinal fibers using the proportioning factor (ξ) as given in Eq. (30).

$$\beta_H = \frac{E_{2t}^{cs}}{E^s} = \frac{\xi E_{1t}^{cs}}{E^s} = \xi \beta_L \quad for\ 0 \leqslant \xi \leqslant 0.80 \tag{30}$$

where 0.80 is the maximum contribution of the hoop fibers which has also been recommended by Imran et al. [60] and 0 is the minimum value, an indication of no contribution of the fibers in the hoop direction. Based on Eq. (30), the proportioning factor (ξ) can be also be expressed as Eq. (31).

$$\xi = \frac{\beta_H}{\beta_L} = \frac{E_{2t}^{cs}}{E_{1t}^{cs}} \tag{31}$$

Once the fibers in the hoop direction are transformed into longitudinal using Eq. (30), it can be assumed that the thickness of fibers in the longitudinal direction (t_L^{cs}) is equal to that of the fibers in the hoop direction (t_H^{cs}). Thus, Eq. (27) takes the form of Eq. (32).

$$t_{es}^{cs} = \beta_L t_L^{cs} (\eta_L + \xi \eta_L) \tag{32}$$

Assuming the non-dimensional fiber reinforcement parameter (α) for which the fibers in hoop direction are considered and using the relation$t_L^{cs} = t_H^{cs}$, Eq. (33) can be formulated.

$$\alpha = \frac{\eta_L t_L^{cs} + \eta_H t_H^{cs}}{t^s} = \frac{(\eta_L + \eta_H) t_L^{cs}}{t^s} \tag{33}$$

From Eq. (33), the thickness of fibers in the longitudinal direction (t_L^{cs}) can be separated as Eq. (34).

$$t_L^{cs} = \frac{\alpha t^s}{\eta_L + \eta_H} \tag{34}$$

By substituting the Eq. (34) into Eq. (32), the thickness of the equivalent section (t_{es}^{cs}) can be written in the normal and non-dimensional forms as Eqs. (35) and (36) respectively.

$$t_{es}^{cs} = \beta_L \left(\frac{\alpha t^s}{\eta_L + \eta_H} \right) (\eta_L + \xi \eta_L) \tag{35}$$

$$\frac{t_{es}^{cs}}{t^s} = \beta_L \left(\frac{\alpha}{\eta_L + \eta_H} \right) (\eta_L + \xi \eta_L) \tag{36}$$

After calculating the thickness of the equivalent section (t_{es}^{cs}), Haedir and Zhao [103] modified the design methods of steel structures given in AS/NZS4600 [153], AS4100 [60] and Eurocode 3 [154]. They concluded that the effect of both the reinforcement factor (α) and the proportioning factor (ξ) should be carefully considered for the effective design of CFRP strengthened steel tubular columns.

5.1.3. Strength prediction under cyclic loads

To account for the effect of quasi-static cyclic loading on the ultimate moment capacity of a CHS under cyclic loads, Tafsirojjaman et al. [76] proposed a strength reduction factor (ϕ_u) of 0.98. The moment capacity of the section can be calculated according to the method proposed by Haedir et al. [39]. They demonstrated the accuracy of their proposed cyclic design factor through comparison with their validated numerical models. A very small value of the coefficient of variation (COV) of 0.047 and a mean ratio of 0.98

indicates that the proposed strength reduction factor can yield accurate results.

5.2. FRP reinforced CHS in aggressive environmental conditions

For structural members used in aggressive environmental conditions, generally, a strength reduction factor (ϕ_u) is proposed which is then multiplied with the service strength to obtain a reduced stren

5.2.1. Prediction models for cold weather conditions

Based on the proposed method of Haedir et al. [39] for CFRP strengthened CHS beams, Kabir et al. [146,147] proposed a strength reduction factor for CHS beams used in cold weather. They conditioned the CFRP strengthened beams at 3 °C of temperature and tested the strengthened beams after 3 and 6 months. They used two types of specimens with and without the surface treatment and proposed that the surfaces must be pre-treated with epoxy to ensure the composite beam action throughout the loading stages. They transformed the FRP section to an equivalent steel section using the method proposed by Haedir et al. [39] but used the fiber strength efficacy (α_m) of 0.5 instead of the proposed 0.19 which is still within the limits of Eq. (3). From their experimental results, they demonstrated that there was a reduction in the detrimental effects of cold weather on the ultimate strength of the beams conditioned for 3 to 6 months. After the comparison of two types of adhesives i.e. MBrace and Araldite [147], they proposed a maximum strength reduction factor (ϕ_u) of 0.90 for CHS beam with epoxy treatment and conditioned for 6 months. Similarly, they proposed an increasing factor (ϕ_s) of 1.20 for deflections of the same beam [146]. The ultimate moment capacity of a compact section in bending can be calculated using Eq. (37).

$$M = F_c \times Z = F_t \times Z \tag{37}$$

whereF_c , Z and F_t are the compressive force, lever arm, and tensile force, respectively. As the cross-section is subjected to bending, compressive stresses are generated in one-half of the cross-section while tensile stresses are generated in the other half. The distribution of compressive and tensile stresses and accompanying strains in the transformed section is shown in Fig. 11. Based on Fig. 11, the areas in compression (A_c) and tension (A_t), compressive (F_c) and tensile (F_t) forces, and the lever arm (Z) can be calculated using Eqs. (38) through (40) respectively.

$$A_c = A_t = \frac{1}{2}\left(A_s + A_{es}^{cs}\right) = \frac{\pi}{2}\left(r_1^2 - r_2^2\right) \tag{38}$$

$$F_c = F_t = A_c \times \sigma_u = A_t \times \sigma_u \tag{39}$$

$$Z = y_1 + y_2 = 2\left[\frac{\frac{\pi r_1^2}{2} \times \frac{4r_1}{3\pi} - \frac{\pi r_2^2}{2} \times \frac{4r_2}{3\pi}}{\frac{\pi}{2}\left(r_1^2 - r_2^2\right)}\right] \tag{40}$$

where A_s and A_{es}^{cs} are the areas of steel and transformed FRP section respectively, r_1 and r_2 are the inner and outer radii of the steel and transformed section respectively, and σ_u is the ultimate steel stress.

5.2.2. Prediction models for marine environments

Although the FRP strengthened steel structures exhibit good durability, their applications in marine environments hinder the utilization of their full strengthened capacities. The factors that influence the effectiveness of FRP strengthening in natural and saline

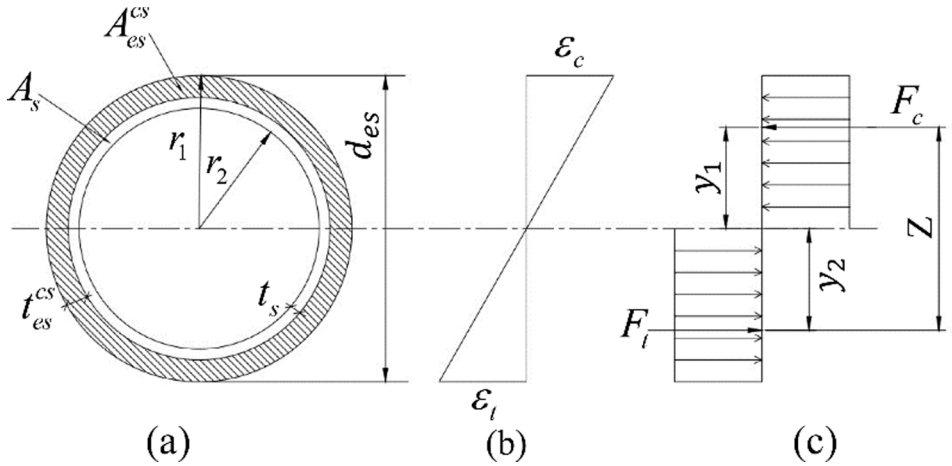

Fig. 11. Stress and strain distributions in the transformed section (a) transformed section (b) strain distribution (c) stress distribution [146].

water environments include high temperature [132,143,155], time, and duration of the exposure [132,156]. To account for the effects of the marine environment on strength degradation, Kabir et al. [142] subjected a CHS to accelerated corrosion to simulate prolonged service life conditions of steel structures. They used a moderate level of corrosion (10% loss of mass) at ambient and 50 °C of temperatures in the saline water conditions (5% NaCl). After keeping the specimens in the accelerated conditions for 25 days, they performed bending tests on the specimens and proposed a strength reduction factor (ϕ_u) of 0.7 for CHS sections strengthened with 3 layers of CFRPs. This strength reduction factor is close to the reduction factor of 0.85 proposed by the Italian codes [24] and economical as compared to the overly conservative equivalent factor of 0.5 in British codes [157].

6. Conclusions

This paper provided a comprehensive review of various techniques to improve the performance and design of steel structures using FRP composite materials. Strength prediction models under a range of loading and environmental conditions have also been provided for effective and safe analysis and design of FRP strengthened steel structures and minimise their failure. From this state-of-the-art review, the following conclusions can be drawn:

- FRP composites with longitudinally oriented fibers are more effective for delaying the onset of local buckling in steel members, however, a combination of longitudinal and hoop fibers is necessary for strengthening against local and global buckling. Also, the FRPs with lower elastic modulus i.e. GFRPs, provide more ductility to the members compared to FRPs that have a higher modulus.
- There are contradicting views and experimental studies are required to ascertain whether the FRPs should be placed closer to the web-flange junction or at the flange tips. For FRPs placed at the flanges or on the webs closer to the web-flange junction to strengthen against local buckling, the shear modulus of FRPs plays a critical role, however, the transverse modulus is critical when FRPs are placed at the mid-height of the webs.
- FRP strengthening effectiveness of steel members prone to flexural buckling depends on the amount of fiber reinforcements, fiber orientations, tensile modulus of the FRPs, and the slenderness of the member. The flexural strength increases with the increase in fiber reinforcements and more longitudinal layers result in more strength while more hoop layers provide more ductility for closed sections. The ultimate capacity also increases with an increase in tensile modulus by a reduction in stresses in the underlying material and deflections are also reduced due to enhanced stiffness.
- Strength enhancement for compression steel members is directly related to the amount of fibers, tensile modulus of fibers, and the slenderness of the plate elements or members and initial imperfections. Hoop-oriented fibers yield better results for short columns while longitudinally oriented fibers provide better strength for the slender elements. Yet, more studies are required, especially on longer columns with slender and non-slender plate elements to determine optimal fiber orientations.
- Strengthening effectiveness for steel members subject to fatigue loads depends on the number of layers, and the longitudinal layers must be confined by additional hoop layers for maximum strength gain. FRPs with higher elastic modulus provide higher stiffness thus reducing stress in the underlying steel elements and impeding the crack growth. Pres-stressing the FRPs for fatigue life improvement is a potential fatigue strengthening improvement technique, however, more studies are required on a range of stress cycles and pre-tensioning levels to better understand and develop guidelines.
- Under impact loads strength of a steel member is increased while its axial and lateral deflections are reduced with the application of FRPs due to increased stiffness. As the modulus of FRPs increases, better strength and reduced deflections are obtained and CFRPs outperform GFRPs due to higher modulus. The strength gain is directly related to the number of FRP layers, and a combination of longitudinal and hoop layers is necessary with more longitudinal layers. Columns with fixed boundary conditions at both ends result in maximum strength gain and the presence of axial pre-load results in strength reduction and increased deflections.
- Strength gain for seismic applications is directly related to the thickness and number of FRP layers as well as the slenderness of the member. FRPs with higher modulus provide higher strength, whereas FRPs with lower modulus result in improved ductility. However, further studies are required on a range of steel sections, orientations of fibers, and different load cycles to gain a greater understanding and develop proper strengthening guidelines.
- The durability of FRP strengthened structures depends on the properties of the adhesive. For marine/seawater conditions, an epoxy adhesive that is thixotropic and has a higher elastic modulus yields better results. An additional layer of GFRP for CFRP strengthened structures that are susceptible to galvanic corrosion can act as an electrical insulator and enhance durability. Yet, further research is required on a range of sections and exposure conditions, especially for FRP strengthened structures in cold weather to develop design guidelines.
- Strength prediction models incorporate the transformed thickness of section from FRP to steel using the modular ratio and the percentage of the fibre strength efficiency relative to steel. Based on the properties of the transformed section, the ultimate capacity of the section can be calculated, and strength reduction factors can be used for varying loading and environmental conditions. The proposed strength reduction factors are 0.90, 0.98, 0.90, and 0.70 for members subjected to compression loads, cyclic loads, cold weather conditions, and marine environment, respectively. However, more studies are needed to confirm the reliability of these strength reduction factors.

Declaration of Competing Interest

The authors declare that they have no known competing financial interests or personal relationships that could have appeared to influence the work reported in this paper.

Acknowledgement

The authors would like to acknowledge the funding provided by National Natural Science Foundation (NSFC 52178097).

References

[1] A.U.R. Dogar, Hafiz Muhammad Ubaid Ur Rehman;, T. Tafsirojjaman;, N. Iqbal;, Experimental investigations on inelastic behaviour and modified Gerber joint for double-span steel trapezoidal sheeting, Structures. 24 (2020) 514–525. 10.1016/j.istruc.2020.01.042.
[2] M. Tavakkolizadeh, H. Saadatmanesh, Fatigue strength of steel girders strengthened with carbon fiber reinforced polymer patch, J. Struct. Eng. 129 (2003) 186–196.
[3] Y. Liu, J.Z. Xie, T. Tafsirojjaman, Q.R. Yue, C. Tan, G.J. Che, CFRP lamella stay-cable and its force measurement based on microwave radar, Case Stud. Constr. Mater. 16 (2022), e00824, https://doi.org/10.1016/j.cscm.2021.e00824.
[4] T. Tafsirojjaman, D.P. Thambiratnam, N.H.R. Sulong, S. Fawzia, Performance of CFRP strengthened full-scale SHS connections subjected to cyclic loading, Thin-Walled Struct. 175 (2022), 109211, https://doi.org/10.1016/j.tws.2022.109211.
[5] Y. Liu, H. Zhang, T. Tafsirojjaman, A. Ur, R. Dogar, O. Alajarmeh, Q. Yue, A. Manalo, A novel technique to improve the compressive strength and ductility of glass fiber reinforced polymer (GFRP) composite bars, Constr. Build. Mater. 326 (2022), 126782, https://doi.org/10.1016/j.conbuildmat.2022.126782.
[6] T. Tafsirojjaman, S. Fawzia, D.P. Thambiratnam, Investigation on the behaviour of CFRP strengthened CHS members under Monotonic loading through finite element modelling, Structures. 28 (2020) 297–308, https://doi.org/10.1016/j.istruc.2020.08.059.
[7] M. Fakri Muda, M. Hisbany Mohd Hashim, M. Khairul Kamarudin, M. Hairil Mohd, T. Tafsirojjaman, M. Abdul Rahman, J. Kee Paik, Burst Pressure Strength of Corroded Subsea Pipelines Repaired with Composite Fiber-Reinforced Polymer Patches, Eng. Fail. Anal. 136 (2022) 106204. https://doi.org/10.1016/j.engfailanal.2022.106204.
[8] A. Al-Fakih, M. Hisbany Mohd Hashim, R. Alyousef, A. Mutafi, S. Hussein Abo Sabah, T. Tafsirojjaman, Cracking behavior of sea sand RC beam bonded externally with CFRP plate, Structures. 33 (2021) 1578–1589. https://doi.org/10.1016/j.istruc.2021.05.042.
[9] S.H. Alsayed, Y.A. Al-Salloum, T.H. Almusallam, Fibre-reinforced polymer repair materials—some facts, in: Proc. Inst. Civ. Eng. Eng., Thomas Telford Ltd, 2000: pp. 131–134.
[10] Y. Duo, X. Liu, Y. Liu, T. Tafsirojjaman, M. Sabbrojjaman, Environmental impact on the durability of FRP reinforcing bars, J. Build. Eng. 43 (2021), 102909, https://doi.org/10.1016/j.jobe.2021.102909.
[11] E. Gudonis, E. Timinskas, V. Gribniak, G. Kaklauskas, A.K. Arnautov, V. Tamulėnas, FRP reinforcement for concrete structures: state-of-the-art review of application and design, Eng. Struct. Technol. 5 (2013) 147–158.
[12] A. Carolin, Carbon fibre reinforced polymers for strengthening of structural elements, Doctoral dissertation, Luleå tekniska universitet (2003).
[13] C. Tuakta, Use of fiber reinforced polymer composite in bridge structures, Doctoral dissertation, Massachusetts Institute of Technology (2005).
[14] P. Banibayat, Experimental investigation of the mechanical and creep rupture properties of basalt fiber reinforced polymer (BFRP) bars, Doctoral dissertation, University of Akron, 2011.
[15] A. Siddika, M.A. Al Mamun, R. Alyousef, Y.H.M. Amran, Strengthening of reinforced concrete beams by using fiber-reinforced polymer composites: A review, J. Build. Eng. 25 (2019), https://doi.org/10.1016/j.jobe.2019.100798.
[16] J.G. Teng, J.-F. Chen, S.T. Smith, L. Lam, FRP: strengthened RC structures, (2002).
[17] K.W. Neale, FRPs for structural rehabilitation: a survey of recent progress, Prog. Struct. Eng. Mater. 2 (2000) 133–138.
[18] D. Oehlers, R. Seracino, Design of FRP and steel plated RC structures: retrofitting beams and slabs for strength, stiffness and ductility, Elsevier, 2004.
[19] S. Rizkalla, T. Hassan, N. Hassan, Design recommendations for the use of FRP for reinforcement and strengthening of concrete structures, Prog. Struct. Eng. Mater. 5 (2003) 16–28.
[20] Y. Liu, T. Tafsirojjaman, A.U.R. Dogar, A. Hückler, Bond behaviour improvement between infra-lightweight and high strength concretes using FRP grid reinforcements and development of bond strength prediction models, Constr. Build. Mater. 270 (2021), 121426, https://doi.org/10.1016/j.conbuildmat.2020.121426.
[21] Y. Liu, T. Tafsirojjaman, A.U.R. Dogar, A. Hückler, Shrinkage behavior enhancement of infra-lightweight concrete through FRP grid reinforcement and development of their shrinkage prediction models, Constr. Build. Mater. 258 (2020), https://doi.org/10.1016/j.conbuildmat.2020.119649.
[22] S.S.J. Moy, FRP composites: life extension and strengthening of metallic structures, Thomas Telford, 2001.
[23] T.C. Miller, M.J. Chajes, D.R. Mertz, J.N. Hastings, Strengthening of a steel bridge girder using CFRP plates, J. Bridg. Eng. 6 (2001) 514–522.
[24] J.M.C. Cadei, T.J. Stratford, L.C. Hollaway, W.G. Dcukett, Strengthening metallic structures using externally bonded fibre-reinforced polymers, Ciria (2004).
[25] F. Yuan, M. Chen, J. Pan, Experimental study on seismic behaviours of hybrid FRP–steel-reinforced ECC–concrete composite columns, Compos. Part B Eng. 176 (2019), 107272.
[26] W. Ge, A.F. Ashour, D. Cao, W. Lu, P. Gao, J. Yu, X. Ji, C. Cai, Experimental study on flexural behavior of ECC-concrete composite beams reinforced with FRP bars, Compos. Struct. 208 (2019) 454–465.
[27] P.M. Stylianidis, M.F. Petrou, Study of the flexural behaviour of FRP-strengthened steel-concrete composite beams, Structures. 22 (2019) 124–138.
[28] Y. Wei, Y. Zhang, J. Chai, G. Wu, Z. Dong, Experimental investigation of rectangular concrete-filled fiber reinforced polymer (FRP)-steel composite tube columns for various corner radii, Compos. Struct. 112311 (2020).
[29] H. Saadatmanesh, Extending service life of concrete and masonry structures with fiber composites, Constr. Build. Mater. 11 (1997) 327–335.
[30] F.G. Carozzi, C. Poggi, E. Bertolesi, G. Milani, Ancient masonry arches and vaults strengthened with TRM, SRG and FRP composites: Experimental evaluation, Compos. Struct. 187 (2018) 466–480.
[31] J.M. Gattas, M.L. O'Dwyer, M.T. Heitzmann, D. Fernando, J.G. Teng, Folded hybrid FRP-timber sections: concept, geometric design and experimental behaviour, Thin-Walled Struct. 122 (2018) 182–192.
[32] L. Min, D. Fernando, B.P. Gilbert, Z. You, Hybrid FRP-timber thin-walled Cee section columns under axial compression: Numerical modelling, Thin-Walled Struct. 157 (2020), 107029.
[33] A. Siddika, M.A. Al Mamun, W. Ferdous, R. Alyousef, Performances, challenges and opportunities in strengthening reinforced concrete structures by using FRPs – A state-of-the-art review, Eng. Fail. Anal. 111 (2020), 104480, https://doi.org/10.1016/j.engfailanal.2020.104480.
[34] L.C. Hollaway, J. Cadei, Progress in the technique of upgrading metallic structures with advanced polymer composites, Prog. Struct. Eng. Mater. 4 (2002) 131–148, https://doi.org/10.1002/pse.112.
[35] A. Shaat, D. Schnerch, A. Fam, S. Rizkalla, Retrofit of steel structures using fiber-reinforced polymers (FRP): State-of-the-art, in, Transp. Res. Board Annu. Meet. (2004).
[36] X.-L. Zhao, L. Zhang, State-of-the-art review on FRP strengthened steel structures, Eng. Struct. 29 (2007) 1808–1823.
[37] J.G. Teng, T. Yu, D. Fernando, Strengthening of steel structures with fiber-reinforced polymer composites, J. Constr. Steel Res. 78 (2012) 131–143, https://doi.org/10.1016/j.jcsr.2012.06.011.
[38] E. Ghafoori, M. Motavalli, Normal, high and ultra-high modulus carbon fiber-reinforced polymer laminates for bonded and un-bonded strengthening of steel beams, J. Mater. Des. 67 (2015) 232–243, https://doi.org/10.1016/j.matdes.2014.11.031.
[39] J. Haedir, M.R. Bambach, X.L. Zhao, R.H. Grzebieta, Strength of circular hollow sections (CHS) tubular beams externally reinforced by carbon FRP sheets in pure bending, Thin-Walled Struct. 47 (2009) 1136–1147, https://doi.org/10.1016/j.tws.2008.10.017.
[40] N.B. Accord, C.J. Earls, Use of Fiber-Reinforced Polymer Composite Elements to Enhance Structural Steel Member Ductility, J. Compos. Constr. 10 (2006) 337–344, https://doi.org/10.1061/(ASCE)1090-0268(2006)10:4(337).

[41] M.A.A. Siddique, A.A. El Damatty, Improvement of local buckling behaviour of steel beams through bonding GFRP plates, Compos. Struct. 96 (2013) 44–56, https://doi.org/10.1016/j.compstruct.2012.08.042.
[42] N. Photiou, L.C. Hollaway, M.K. Chryssanthopoulos, Strengthening Of An Artificially Degraded Steel Beam Utilising A Carbon/Glass Composite System, Adv. Polym. Compos. Struct. Appl. Constr. ACIC 2004 (20) (2004) 274–283, https://doi.org/10.1016/B978-1-85573-736-5.50030-3.
[43] M.H. Kabir, S. Fawzia, T.H.T. Chan, J.C.P.H. Gamage, J.B. Bai, Experimental and numerical investigation of the behaviour of CFRP strengthened CHS beams subjected to bending, Eng. Struct. 113 (2016) 160–173, https://doi.org/10.1016/j.engstruct.2016.01.047.
[44] M.H. Kabir, S. Fawzia, T.H.T. Chan, Effects of layer orientation of CFRP strengthened hollow steel members, Gradjevinar. 67 (2015) 441–450, https://doi.org/10.14256/JCE.1127.2014.
[45] M.J. Altaee, L.S. Cunningham, M. Gillie, Experimental investigation of CFRP-strengthened steel beams with web openings, J. Constr. Steel Res. 138 (2017) 750–760, https://doi.org/10.1016/j.jcsr.2017.08.023.
[46] P. Colombi, C. Poggi, An experimental, analytical and numerical study of the static behavior of steel beams reinforced by pultruded CFRP strips, Compos. Part B Eng. 37 (2006) 64–73, https://doi.org/10.1016/j.compositesb.2005.03.002.
[47] S. Selvaraj, M. Madhavan, CFRP strengthened steel beams : Improvement in failure modes and performance analysis, Structures. 12 (2017) 120–131, https://doi.org/10.1016/j.istruc.2017.08.008.
[48] T.W. Siwowski, P. Siwowska, Experimental study on CFRP-strengthened steel beams, Compos. Part B Eng. 149 (2018) 12–21.
[49] M.V. Seica, J.A. Packer, FRP materials for the rehabilitation of tubular steel structures, for underwater applications, Compos. Struct. 80 (2007) 440–450, https://doi.org/10.1016/j.compstruct.2006.05.029.
[50] A.A. El Damatty, M. Abushagur, M.A. Youssef, Experimental and analytical investigation of steel beams rehabilitated using GFRP sheets, Steel Compos. Struct. 3 (2003) 421–438, https://doi.org/10.12989/scs.2003.3.6.421.
[51] J. Haedir, M.R. Bambach, X.L. Zhao, R.H. Grzebieta, Bending strength of CFRP-strengthened circular hollow steel sections, in: Int. Conf. FRP Compos. Civ. Eng. 2006, Florida International University, 2006: pp. 701–704.
[52] J. Haedir, M.R. Bambach, X.L. Zhao, R.H. Grzebieta, Behaviour of thin-walled CHS beams reinforced by CFRP sheets, in: Int. Struct. Eng. Constr. Conf. 2007, Taylor & Francis, 2007: pp. 701–706.
[53] A. Punitha Kumar, R. Senthil, Behavior of CFRP strengthened CHS under axial static and axial cyclic loading, KSCE J. Civ. Eng. 20 (2016) 1493–1500, https://doi.org/10.1007/s12205-015-0151-4.
[54] Q. Wu, X. Zhi, Experimental and numerical study of GFRP-reinforced circular steel tube under axial compression, J. Constr. Steel Res. 168 (2020), 105990, https://doi.org/10.1016/j.jcsr.2020.105990.
[55] A. Shaat, A. Fam, Fiber-element model for slender HSS columns retrofitted with bonded high-modulus composites, J. Struct. Eng. 133 (2007) 85–95, https://doi.org/10.1061/(ASCE)0733-9445(2007)133:1(85).
[56] A. Ritchie, A. Fam, C. MacDougall, Strengthening long steel columns of S-sections against global buckling around weak axis using CFRP plates of various moduli, J. Compos. Constr. 19 (2015) 1–11, https://doi.org/10.1061/(ASCE)CC.1943-5614.0000534.
[57] M.R. Bambach, H.H. Jama, M. Elchalakani, Axial capacity and design of thin-walled steel SHS strengthened with CFRP, Thin-Walled Struct. 47 (2009) 1112–1121, https://doi.org/10.1016/j.tws.2008.10.006.
[58] A. Shaat, A. Fam, Axial loading tests on short and long hollow structural steel columns retrofitted using carbon fibre reinforced polymers, Can. J. Civ. Eng. 33 (2006) 458–470, https://doi.org/10.1139/L05-042.
[59] A. Shaat, A.Z. Fam, Slender steel columns strengthened using high-modulus CFRP plates for buckling control, J. Compos. Constr. 13 (2009) 2–12, https://doi.org/10.1061/(ASCE)1090-0268(2009)13:1(2).
[60] M. Imran, M. Mahendran, P. Keerthan, Experimental and numerical investigations of CFRP strengthened short SHS steel columns, Eng. Struct. 175 (2018) 879–894, https://doi.org/10.1016/j.engstruct.2018.08.042.
[61] M.I. Alam, S. Fawzia, Numerical studies on CFRP strengthened steel columns under transverse impact, Compos. Struct. 120 (2015) 428–441, https://doi.org/10.1016/j.compstruct.2014.10.022.
[62] M.I. Alam, S. Fawzia, X.L. Zhao, A.M. Remennikov, Experimental Study on FRP-Strengthened Steel Tubular Members under Lateral Impact, J. Compos. Constr. 21 (2017), https://doi.org/10.1061/(ASCE)CC.1943-5614.0000801.
[63] M. Kadhim, Z. Wu, L. Cunningham, Modelling impact resistance of polymer-laminated steelwork, Proc. Inst. Civ. Eng. Eng. Comput. Mech. 170 (2017) 7–24, https://doi.org/10.1680/jencm.15.00018.
[64] C. Batuwitage, S. Fawzia, D. Thambiratnam, X. Liu, R. Al-Mahaidi, M. Elchalakani, Impact behaviour of carbon fibre reinforced polymer (CFRP) strengthened square hollow steel tubes: A numerical simulation, Thin-Walled Struct. 131 (2018) 245–257, https://doi.org/10.1016/j.tws.2018.06.033.
[65] C. Batuwitage, S. Fawzia, D.P. Thambiratnam, T. Tafsirojjaman, R. Al-Mahaidi, M. Elchalakani, CFRP-wrapped hollow steel tubes under axial impact loading, in: Tubul. Struct. XVI Proc. 16th Int. Symp. Tubul. Struct. (ISTS 2017, 4-6 December 2017, Melbourne, Aust., CRC Press, 2017: pp. 401–408.
[66] M.I. Alam, S. Fawzia, T. Tafsirojjaman, X.L. Zhao, FE modeling of FRP strengthened CHS members subjected to lateral impact, in: Tubul. Struct. XVI Proc. 16th Int. Symp. Tubul. Struct. (ISTS 2017, 4-6 December 2017, Melbourne, Aust., CRC Press, 2017: pp. 409–414.
[67] M.M.A. Kadhim, Z. Wu, L.S. Cunningham, Experimental and Numerical Investigation of CFRP-Strengthened Steel Beams under Impact Load, J. Struct. Eng. (United States). 145 (2019), https://doi.org/10.1061/(ASCE)ST.1943-541X.0002288.
[68] M.I. Alam, S. Fawzia, X.-L. Zhao, A.M. Remennikov, Numerical Modeling and Performance Assessment of FRP-Strengthened Full-Scale Circular-Hollow-Section Steel Columns Subjected to Vehicle Collisions, J. Compos. Constr. 24 (2020) 04020011, https://doi.org/10.1061/(asce)cc.1943-5614.0001011.
[69] H. Al-Zubaidy, R. Al-Mahaidi, X.L. Zhao, Experimental investigation of bond characteristics between CFRP fabrics and steel plate joints under impact tensile loads, Compos. Struct. 94 (2012) 510–518, https://doi.org/10.1016/j.compstruct.2011.08.018.
[70] H. Al-Zubaidy, R. Al-Mahaidi, X.L. Zhao, Finite element modelling of CFRP/steel double strap joints subjected to dynamic tensile loadings, Compos. Struct. 99 (2013) 48–61, https://doi.org/10.1016/j.compstruct.2012.12.003.
[71] T. Tafsirojjaman, S. Fawzia, D. Thambiratnam, X.L. Zhao, Seismic strengthening of rigid steel frame with CFRP, Arch. Civ. Mech. Eng. 19 (2019) 334–347, https://doi.org/10.1016/j.acme.2018.08.007.
[72] T. Tafsirojjaman, S. Fawzia, D. Thambiratnam, X.L. Zhao, Behaviour of CFRP strengthened CHS members under monotonic and cyclic loading, Compos. Struct. 220 (2019) 592–601, https://doi.org/10.1016/j.compstruct.2019.04.029.
[73] T. Tafsirojjaman, S. Fawzia, D. Thambiratnam, Numerical investigation on the seismic strengthening of steel frame by using normal and high modulus CFRP, in: D.F. and Z.Y.W. S.T. Smith, T. Yu (Ed.), Seventh Asia-Pacific Conf. FRP Struct. (APFIS 2019) Surfers Parad. Gold Coast, Aust. 10-13 December, 2019: pp. 10–13.
[74] T. Tafsirojjaman, S. Fawzia, D. Thambiratnam, Numerical investigation on the cfrp strengthened steel frame under earthquake, Mater. Sci. Forum. 995 (2020) 123–129, https://doi.org/10.4028/www.scientific.net/MSF.995.123.
[75] S. Tafsirojjaman, D. Fawzia, Thambiratnam, Enhancement of Seismic Performance of Steel Frame through CFRP Strengthening, Procedia Manuf. 30 (2019) 239–246.
[76] T. Tafsirojjaman, S. Fawzia, D.P. Thambiratnam, X.L. Zhao, Study on the cyclic bending behaviour of CFRP strengthened full-scale CHS members, Structures. 28 (2020) 741–756, https://doi.org/10.1016/j.istruc.2020.09.015.
[77] T. Tafsirojjaman, S. Fawzia, D. Thambiratnam, X. Zhao, Numerical investigation of CFRP strengthened RHS members under cyclic loading, Structures. 24 (2020) 610–626, https://doi.org/10.1016/j.istruc.2020.01.041.
[78] T. Tafsirojjaman, S. Fawzia, D.P. Thambiratnam, Structural behaviour of CFRP strengthened beam-column connections under monotonic and cyclic loading, Structures. 33 (2021) 2689–2699, https://doi.org/10.1016/j.istruc.2021.06.028.
[79] B.T.C. Miller, M.J. Chajes, D.R. Mertz, J.N. Hastings, S. Member, Cfrp p, J. Bridg. Eng. 6 (2001) 514–522, https://doi.org/10.1061/(ASCE)1084-0702(2001)6.
[80] M. Tavakkolizadeh, M. Asce, H. Saadatmanesh, M. Asce, Fatigue Strength of Steel Girders Strengthened with Carbon Fiber Reinforced Polymer Patch, 129 (2003) 186–196.

[81] H. Liu, R. Al-mahaidi, X. Zhao, Experimental study of fatigue crack growth behaviour in adhesively reinforced steel structures, Compos. Struct. 90 (2009) 12–20, https://doi.org/10.1016/j.compstruct.2009.02.016.
[82] R.J. Dexter, J.M. Ocel, Manual for Repair and Retrofit of Fatigue Cracks in Steel Bridges (FHWA-IF-13-020), Fed. Highw. Adm. (2013) 134.
[83] H. Nakamura, W. Jiang, H. Suzuki, Maeda, T. Irube, Experimental study on repair of fatigue cracks at welded web gusset joint using CFRP strips, Thin-Walled Struct. 47 (2009) 1059–1068. https://doi.org/10.1016/j.tws.2008.10.016.
[84] C. Wu, X.L. Zhao, R. Al-Mahaidi, M.R. Emdad, W.H. Duan, Fatigue tests on steel plates with longitudinal weld attachment strengthened by ultra high modulus carbon fibre reinforced polymer plate, Fatigue Fract. Eng. Mater. Struct. 36 (2013) 1027–1038, https://doi.org/10.1111/ffe.12067.
[85] L. Hu, P. Feng, X. Zhao, Thin-Walled Structures Fatigue design of CFRP strengthened steel members, Thin Walled Struct. 119 (2017) 482–498, https://doi.org/10.1016/j.tws.2017.06.029.
[86] F.R. Mashiri, X.L. Zhao, Fatigue tests and design of welded thin-walled RHS-RHS and RHS-angle cross-beam connections under cyclic bending, Thin-Walled Struct. 48 (2010) 159–168, https://doi.org/10.1016/j.tws.2009.07.006.
[87] B.M. Imam, M.K. Chryssanthopoulos, A review of metallic bridge failure statistics, Bridg. Maintenance, Safety, Manag. Life-Cycle Optim. - Proc. 5th Int. Conf. Bridg. Maintenance, Saf. Manag. (2010) 3281–3288, https://doi.org/10.1201/b10430-502.
[88] A.H. Al-Saidy, F.W. Klaiber, T.J. Wipf, Repair of Steel Composite Beams with Carbon Fiber-Reinforced Polymer Plates, J. Compos. Constr. 8 (2004) 163–172, https://doi.org/10.1061/(asce)1090-0268(2004)8:2(163).
[89] W.T. Segui, Steel design, Cengage Learning, 2012.
[90] L.S. Da Silva, R. Simões, H. Gervásio, Design of Steel Structures: Eurocode 3: Design of Steel Structures, Part 1-1: General Rules and Rules for Buildings, John Wiley & Sons, 2012.
[91] American Institute of Steel Construction, Specification for Structural Steel Buildings, ANSI / AISC 360-16, Am. Inst. Steel Constr. (2016) 676.
[92] CEN (European Committee for Standardization), Eurocode 3: Design of steel structures—Part 1-1: General rules and rules for buildings, (2005).
[93] E. Ekiz, S. El-Tawil, G. Parra-Montesinos, S. Goel, Enhancing plastic hinge behavior in steel flexural members using CFRP wraps, in: Proc., 13th World Conf. Earthq. Eng., Vancouver, 2004.
[94] E. Sayed-Ahmad, Strengthening of Thin-Walled Steel I-Section Beams Using Cfrp Strips, 4th Int, Conf. Adv. Compos. Mater. Bridg. Struct. 4 (2004) 1–8.
[95] S. El-Tawil, E. Ekiz, S. Goel, S.H. Chao, Retraining local and global buckling behavior of steel plastic hinges using CFRP, J. Constr. Steel Res. 67 (2011) 261–269, https://doi.org/10.1016/j.jcsr.2010.11.007.
[96] K.A. Harries, Enhancing the stability of structural steel components using fibre-reinforced polymer (FRP) composites, Woodhead Publishing Limited (2014), https://doi.org/10.1533/9780857096654.2.117.
[97] W.F. Ragheb, Inelastic Local Buckling and Rotation Capacity of Steel I-Beams Strengthened with Bonded FRP Sheets, J. Compos. Constr. 21 (2017) 04016058, https://doi.org/10.1061/(asce)cc.1943-5614.0000716.
[98] W.F. Ragheb, Elastic local buckling of steel I-sections strengthened with bonded FRP strips, J. Constr. Steel Res. 107 (2015) 81–93, https://doi.org/10.1016/j.jcsr.2015.01.009.
[99] T. Tafsirojjaman, S. Fawzia, D.P. Thambiratnam, N. Wirth, Performance of FRP strengthened full-scale simply-supported circular hollow steel members under monotonic and large-displacement cyclic loading, Eng. Struct. 242 (2021), 112522, https://doi.org/10.1016/j.engstruct.2021.112522.
[100] H.A. Rasheed, H. Ahmadi, A.E. Abouelleil, Lateral-torsional buckling of simply supported anisotropic steel-FRP rectangular beams under pure bending condition, Eng. Struct. 146 (2017) 127–139, https://doi.org/10.1016/j.engstruct.2017.05.037.
[101] K. Deng, P. Pan, X. Nie, X. Xu, P. Feng, L. Ye, Study of GFRP steel buckling restraint braces, J. Compos. Constr. 19 (2015) 4015009.
[102] N. Trahair, M.A. Bradford, Behaviour and Design of Steel Structures to AS4100: Australian, CRC Press, 2017.
[103] J. Haedir, X.L. Zhao, Design of short CFRP-reinforced steel tubular columns, J. Constr. Steel Res. 67 (2011) 497–509, https://doi.org/10.1016/j.jcsr.2010.09.005.
[104] J.G. Teng, Y.M. Hu, Behaviour of FRP-jacketed circular steel tubes and cylindrical shells under axial compression, Constr. Build. Mater. 21 (2007) 827–838.
[105] X.G. Wang, J.A. Bloch, D. Cesari, Axial crushing of tubes made of multi-materials, Mech. Mech. Damage Compos. Multi Mater. 1 (1991) 351–361.
[106] A. Shaat, A. Fam, Strengthening of short HSS steel columns using FRP sheets, in: Proc. 4th Int. Conf. Adv. Compos. Mater. Bridg. Struct., 2004.
[107] P. Colombi, G. Fava, Fatigue crack growth in steel beams strengthened by CFRP strips, Theor. Appl. Fract. Mech. 85 (2016) 173–182, https://doi.org/10.1016/j.tafmec.2016.01.007.
[108] P. Colombi, A. Bassetti, A. Nussbaumer, Crack growth induced delamination on steel members reinforced by prestressed composite patch, Fatigue Fract. Eng. Mater. Struct. 26 (2003) 429–438.
[109] S.C. Jones, S.A. Civjan, Application of fiber reinforced polymer overlays to extend steel fatigue life, J. Compos. Constr. 7 (2003) 331–338.
[110] P. Feng, L. Hu, X.-L. Zhao, L. Cheng, S. Xu, Study on thermal effects on fatigue behavior of cracked steel plates strengthened by CFRP sheets, Thin-Walled Struct. 82 (2014) 311–320, https://doi.org/10.1016/j.tws.2014.04.015.
[111] L.L. Hu, X.L. Zhao, P. Feng, Fatigue behavior of cracked high-strength steel plates strengthened by CFRP sheets, J. Compos. Constr. 20 (2016) 4016043.
[112] J. Deng, M.M.K. Lee, Fatigue performance of metallic beam strengthened with a bonded CFRP plate, Compos. Struct. 78 (2007) 222–231.
[113] T. Chen, Y. Qian-Qian, G. Xiang-lin, Study on fatigue behavior of strengthened non-load-carrying cruciform welded joints using carbon fiber sheets, 12 (2012) 179–194. https://doi.org/10.1142/S0219455412004586.
[114] Q.R. Yue, Y. Zheng, X. Chen, X.G. Liu, Research on fatigue performance of CFRP reinforced steel crane girder, Compos. Struct. 154 (2016) 277–285, https://doi.org/10.1016/j.compstruct.2016.07.066.
[115] P. Colombi, A. Bassetti, A. Nussbaumer, Analysis of cracked steel members reinforced by pre-stress composite patch, Fatigue Fract. Eng. Mater. Struct. 26 (2003) 59–66.
[116] H. Liu, Z. Xiao, X.L. Zhao, R. Al-Mahaidi, Prediction of fatigue life for CFRP-strengthened steel plates, Thin-Walled Struct. 47 (2009) 1069–1077, https://doi.org/10.1016/j.tws.2008.10.011.
[117] B. Täljsten, C.S. Hansen, J.W. Schmidt, Strengthening of old metallic structures in fatigue with prestressed and non-prestressed CFRP laminates, Constr. Build. Mater. 23 (2009) 1665–1677, https://doi.org/10.1016/j.conbuildmat.2008.08.001.
[118] A. Al-Mosawe, R. Al-Mahaidi, X.L. Zhao, Experimental and Numerical Study on Strengthening of Steel Members Subjected to Impact Loading Using Ultrahigh Modulus CFRP, J. Compos. Constr. 20 (2016) 1–10, https://doi.org/10.1061/(ASCE)CC.1943-5614.0000703.
[119] H.-L. Hsu, Z.-C. Li, Seismic performance of steel frames with controlled buckling mechanisms in knee braces, J. Constr. Steel Res. 107 (2015) 50–60.
[120] J. Jim, J. Park, Design of steel moment frames considering progressive collapse, Steel Compos. Struct. 8 (2008) 85–98, https://doi.org/10.1007/s13296-014-2013-1.
[121] D. Dubina, A. Stratan, Behaviour of welded connections of moment resisting frames beam-to-column joints, Eng. Struct. 24 (2002) 1431–1440, https://doi.org/10.1016/S0141-0296(02)00091-3.
[122] P.D. Moncarz, B.M. McDonald, R.D. Caligiuri, Earthquake failures of welded building connections, Int. J. Solids Struct. 38 (2001) 2025–2032, https://doi.org/10.1016/S0020-7683(00)00150-5.
[123] S. a. Mahin, Lessons from damage to steel buildings during the Northridge earthquake, Eng. Struct. 20 (1998) 261–270. https://doi.org/10.1016/S0141-0296(97)00032-1.
[124] K.C. Tsai, S. Wu, Behavior and design of seismic moment resisting beam-column joints, Center for Earthquake Engineering Research, National Taiwan University, 1993.
[125] K.C. Lin, K.C. Tsai, H.Y. Chang, Failure Modes and Flexural Ductility of Steel Moment Connections, Main (2008).
[126] Y.-J. Kim, S.-H. Oh, T.-S. Moon, Seismic behavior and retrofit of steel moment connections considering slab effects, Eng. Struct. 26 (2004) 1993–2005.
[127] T. Kim, A.S. Whittaker, A.S.J. Gilani, V.V. Bertero, S.M. Takhirov, Cover-plate and flange-plate steel moment-resisting connections, J. Struct. Eng. 128 (2002) 474–482.
[128] N.D. Fernando, Bond behaviour and debonding failures in CFRP-strengthened steel members, (2011).

[129] Z.-G. Xiao, X.-L. Zhao, CFRP repaired welded thin-walled cross-beam connections subject to in-plane fatigue loading, Int. J. Struct. Stab. Dyn. 12 (2012) 195–211.
[130] T. Tafsirojjaman, S. Fawzia, D. Thambiratnam, X.L. Zhao, FRP strengthened SHS beam-column connection under monotonic and large-deformation cyclic loading, Thin-Walled Struct. 161 (2021), 107518, https://doi.org/10.1016/j.tws.2021.107518.
[131] J.R. Cromwell, K.A. Harries, B.M. Shahrooz, Environmental durability of externally bonded FRP materials intended for repair of concrete structures, Constr. Build. Mater. 25 (2011) 2528–2539.
[132] T.-C. Nguyen, Y. Bai, X.-L. Zhao, R. Al-Mahaidi, Durability of steel/CFRP double strap joints exposed to sea water, cyclic temperature and humidity, Compos. Struct. 94 (2012) 1834–1845.
[133] V.M. Karbhari, S.B. Shulley, Use of composites for rehabilitation of steel structures—determination of bond durability, J. Mater. Civ. Eng. 7 (1995) 239–245.
[134] P. Colombi, E. Fanesi, G. Fava, C. Poggi, Durability of steel elements strengthened by FRP plates subjected to mechanical and environmental loads, in: Proc. 3rd Int. Conf. Compos. Constr., 2005: pp. 291–298.
[135] A. Pizzi, K.L. Mittal, Handbook of adhesive technology, CRC press, 2017.
[136] F.E. Sloan, J.B. Talbot, Corrosion of graphite-fiber-reinforced composites I—Galvanic coupling damage, Corrosion. 48 (1992) 830–838.
[137] W.C. Tucker, R. Brown, Blister formation on graphite/polymer composites galvanically coupled with steel in seawater, J. Compos. Mater. 23 (1989) 389–395.
[138] M. Tavakkolizadeh, H. Saadatmanesh, Galvanic corrosion of carbon and steel in aggressive environments, J. Compos. Constr. 5 (2001) 200–210.
[139] D.R. Mertz, J.W. Gillespie, Rehabilitation of steel bridge girders through the application of advanced composite materials, 1996.
[140] R. Francis, Bimetallic corrosion: Guides to good practice in corrosion control, Teddington, Middlesex Natl. Phys. Lab. Retrieved July. 14 (2000) 2008.
[141] J.W. Gillespie Jr, T.D. West, Enhancements to the bond between advanced composite materials and steel for bridge rehabilitation, 2002.
[142] M.H. Kabir, S. Fawzia, T.H.T. Chan, M. Badawi, Durability of CFRP strengthened steel circular hollow section member exposed to sea water, Constr. Build. Mater. 118 (2016) 216–225, https://doi.org/10.1016/j.conbuildmat.2016.04.087.
[143] M. Dawood, S. Rizkalla, Environmental durability of a CFRP system for strengthening steel structures, Constr. Build. Mater. 24 (2010) 1682–1689, https://doi.org/10.1016/j.conbuildmat.2010.02.023.
[144] M.H. Kabir, S. Fawzia, T.H.T. Chan, M. Badawi, Numerical studies on CFRP strengthened steel circular members under marine environment, Mater. Struct. 49 (2016) 4201–4216, https://doi.org/10.1617/s11527-015-0781-5.
[145] C. Batuwitage, S. Fawzia, D. Thambiratnam, R. Al-Mahaidi, Durability of CFRP strengthened steel plate double-strap joints in accelerated corrosion environments, Compos. Struct. 160 (2017) 1287–1298, https://doi.org/10.1016/j.compstruct.2016.10.101.
[146] M.H. Kabir, S. Fawzia, T.H.T. Chan, J.C.P.H. Gamage, Durability performance of carbon fibre-reinforced polymer strengthened circular hollow steel members under cold weather, Aust. J. Struct. Eng. 15 (2014) 377–392, https://doi.org/10.7158/13287982.2014.11465172.
[147] M.H. Kabir, S. Fawzia, T.H.T. Chan, J.C.P.H. Gamage, Comparative durability study of CFRP strengthened tubular steel members under cold weather, Mater. Struct. 49 (2016) 1761–1774, https://doi.org/10.1617/s11527-015-0610-x.
[148] M.H. Kabir, S. Fawzia, T.H.T. Chan, Durability of CFRP strengthened circular hollow steel members under cold weather: Experimental and numerical investigation, Constr. Build. Mater. 123 (2016) 372–383, https://doi.org/10.1016/j.conbuildmat.2016.06.116.
[149] A. Australian Standard, Steel structures, (1998).
[150] M. Seica, J. Packer, P. Ramirez, S. Bell, X. Zhao, Rehabilitation of tubular members with carbon reinforced polymers, in: Tubul. Struct. XI 11th Int. Symp. IIW Int. Conf. Tubul. Struct., CRC Press, 2006: p. 365.
[151] American Iron and Steel Institute, North American specification for the design of cold-formed steel structural members, American Iron & Steel Institute, Committee of Steel Plate Producers …, 2007.
[152] K.S. Pister, S.B. Dong, Elastic bending of layered plates, J. Eng. Mech. Div. 85 (1959) 1–10.
[153] AS/NZS 4600, Cold-formed steel structures, (2005).
[154] EN 1999-Eurocode 9: Design of aluminium structures, (2007).
[155] T.-C. Nguyen, Y. Bai, X.-L. Zhao, R. Al-Mahaidi, Curing effects on steel/CFRP double strap joints under combined mechanical load, temperature and humidity, Constr. Build. Mater. 40 (2013) 899–907.
[156] M.R. Bowditch, The durability of adhesive joints in the presence of water, Int. J. Adhes. Adhes. 16 (1996) 73–79.
[157] CNR-DT 202/2005, Guidelines for the Design and Construction of Externally Bonded FRP Systems for Strengthening Existing Structures, Metallic structures, Natl. Res. Counc. Advis. Comm. Tech. Recomm. Constr. (2007).